Fig. 3. Immunohistochemistry for ATF3, phosphorylated c-Jun (p-c-Jun), phosphorylated Hsp27 (p-Hsp27), and GFAP of facial nuclei in H46R-tg rat, G93A-tg rat, and non-tg littermate on the ipsilateral (avulsion or axotomy) and contralateral sides 2 weeks after facial nerve avulsion or axotomy. All injured motoneurons are immuno-stained for ATF3, phosphorylated c-Jun, and phosphorylated Hsp27 in these rats after avulsion or axotomy. The intensity of GFAP immunoreactivity appears parallel to the extent of motoneuron loss (see also Fig. 1). Counterstained with hematoxylin. Scale bar = 50 μm.

study, we did not observe immunoreactivity for SOD1 in facial motoneurons of nontransgenic littermates with sheep and rabbit anti-human SOD1 antibodies; it is postulated that the antibody concentrations (i.e., 1:1,000–10,000) used in this study are below the detection levels for immunostaining rat SOD1 antigen on paraffin sections. Instead, we demonstrated some facial motoneurons showing very faint immunoreactivity for SOD1 in H46R-tg rats on paraffin sections. In G93A-tg rats, axons and vacuoles in neuropil were intensely immunoreactive for SOD1 at both uninjured and injured sides. The increased immunostaining for SOD1 in injured motoneurons of SOD1 (H46R and G93A)-tg rats may therefore indicate that human mutant SOD1 protein is accumulated in the cytoplasm of facial motoneurons after avulsion. When several mutant SOD1 genes that include G93A were transfected to COS7 cells, the mutant SOD1s, but not wild-type SOD1, aggregated in association with the endoplasmic reticulum (ER) and induced ER stress (Tobisawa et al., 2003). Accumulation of mutant SOD1 in injured motoneurons after avulsion may therefore potentiate ER stress and exacerbate motoneuron death in the presymptomatic mutant SOD1-tg rats, although the mechanism of accumulation of SOD1 remains unknown. Whether up-regulation of cytoplasmic mutant SOD1 expression or retrograde accumulation of mutant SOD1 from injured axons was induced in these neurons awaits further investigations. In addition, facial nerve axotomy, as opposed to avulsion, did not increase immunoreactivity for SOD1 in injured motoneurons of SOD1-tg rats and their non-tg littermates, which seems consistent with the absence of significant motoneuron loss in these rats as described above. As for wild-type SOD1, previous reports documented no change in SOD1 mRNA levels or SOD1 immunoreactivity in injured motoneurons after facial or sciatic nerve axotomy in wild-type rats (Yoneda et al., 1992; Rosefeld et al., 1997).

It has been demonstrated that ATF3 is expressed, and c-Jun and Hsp27 are up-regulated and phosphorylated, in injured adult motoneurons after axotomy (Tsujino et al., 2000; Casanovas et al., 2001; Benn et al., 2002; Kalmár et al., 2002). As for the neuroprotective nature of these molecules, it has been reported that ATF3 enhances c-Jun-mediated neurite sprouting in PC12 and Neuro-2a cells (Pearson et al., 2003), and ATF3 and Hsp27 cooperate with c-Jun to prevent death of PC12 cells and superior cervical ganglion neurons (Nakagomi et al., 2003). Hsp27 is induced and phosphorylated in adult, but not in neonatal, motoneurons after axotomy, and axotomized neonatal motoneurons that lack Hsp27 die by apoptosis, suggesting that phosphorylated Hsp27 is necessary for motoneuron survival after peripheral nerve injury (Benn et al., 2002). However, there have been no reports concerning the expression of ATF3, phosphorylated c-Jun, and phosphorylated Hsp27 in injured motoneurons after avulsion. In the present study, we have demonstrated that, even after avulsion that causes extensive motoneuron death, ATF3,

phosphorylated c-Jun, and phosphorylated Hsp27 were fully up-regulated in both SOD1-tg and non-tg rats. These results suggest that neuroprotective effects of Hsp27 cannot overcome yet unidentified stress(es) induced by facial nerve avulsion. On the other hand, a recent report demonstrated that facial motoneurons of c-Jun-deficient mice are resistant to axotomy-induced cell death, suggesting that c-Jun promotes posttraumatic motoneuron death (Raivich et al., 2004). In addition, it has been shown that mutant SOD1 binds to Hsp27 and forms aggregates, suggesting that this binding of Hsp27 to mutant SOD1 blocks antiapoptotic function of Hsp27 and leads to motoneuron death (Okado-Matsumoto and Fridovich, 2002). The effects of phosphorylated c-Jun and Hsp27 and their association with mutant SOD1 accumulation should be further investigated to elucidate the mechanism of exacerbated motoneuron death in SOD1-tg rats after avulsion.

In this study, we have demonstrated that motoneuron degeneration after facial nerve avulsion is exacerbated in presymptomatic mutant SOD1-tg rats compared with their non-tg littermates. Mutant SOD1 accumulation and its association with c-Jun and Hsp27 may have a key role leading to enhanced motoneuron death. In this context, motoneuron death after avulsion may share, at least in part, a common mechanism with the motoneuron degeneration associated with SOD1 mutation.

ACKNOWLEDGMENT

REFERENCES

Angelov DN, Waibel S, Guntinas-Lichius O, Lenzen M, Neiss WF, Tomov TL, Yoles E, Kipnis J, Schori H, Reuter A, Ludolph A, Schwartz M. 2003. Therapeutic vaccine for acute and chronic motor neuron diseases: implications for amyotrophic lateral sclerosis. Proc Natl Acad Sci U S A 100:4790–4795.

Aoki M, Ogasawara M, Matsubara Y, Narisawa K, Nakamura S, Itoyama Y, Abe K. 1993. Mild ALS in Japan associated with novel SOD mutation. Nat Genet 5:323–324.

Aoki M, Ogasawara M, Matsubara Y, Narisawa K, Nakamura S, Itoyama Y, Abe K. 1994. Familial amyotrophic lateral sclerosis (ALS) in Japan associated with H46R mutation in Cu/Zn superoxide dismutase gene: a possible new subtype of familial ALS. J Neurol Sci 126:77–83.

Asayama K, Burr IM. 1984. Joint purification of mangano and copper/zinc superoxide dismutase from a single source: a simplified method. Anal Biochem 136:336–339.

Benn SC, Perrelet D, Kato AC, Scholz J, Decosterd I, Mannion RJ, Bakowska JC, Woolf CJ. 2002. Hsp27 upregulation and phosphorylation is required for injured sensory and motor neuron survival. Neuron 36:45–56.

Casanovas A, Ribera J, Hager G, Kreutzberg GW, Esquerda JE. 2001. c-Jun regulation in rat neonatal motoneurons postaxotomy. J Neurosci 63:469–479.

Cleveland DW. 1999. From Charcot to SOD1: mechanisms of selective motor neuron death in ALS. Neuron 24:515–520.

Cleveland DW, Rothstein JD. 2001. From Charcot to Lou Gehrig: deciphering selective motor neuron death in ALS. Nat Rev Neurosci 2:806–819.

Estévez AG, Spear N, Manuel SM, Barbeito L, Radi R, Beckman JS. 1998. Role of endogenous nitric oxide and peroxynitrite formation in the survival and death of motor neurons in culture. Prog Brain Res 18: 269–280.

Hottinger AF, Azzouz M, Déglon N, Aebischer P, Zurn AD. 2000. Complete and long-term rescue of lesioned adult motoneurons by lentiviral-mediated expression of glial cell line-derived neurotrophic factor in the facial nucleus. J Neurosci 20:5587–5593.

Ikeda K, Sakamoto T, Kawazoe Y, Marubuchi S, Nakagawa M, Ono S, Terashima N, Kinoshita M, Iwasaki Y, Watabe K. 2003. Oral administration of a neuroprotective compound T-588 prevents motoneuron degeneration after facial nerve avulsion in adult rats. Amyotroph Lateral Scler Other Motor Neuron Disord 4:74–80.

Kalmár B, Burnstock G, Vrborá G, Greensmith L. 2002. The effect of neonatal injury on the expression of heat shock proteins in developing rat motoneurons. J Neurotrauma 19:667–679.

Koliatsos VE, Price DL. 1996. Axotomy as an experimental model of neuronal injury and cell death. Brain Pathol 6:447–465.

Koliatsos VE, Applegate MD, Kitt CA, Walker LC, DeLong MR, Price DL. 1989. Aberrant phosphorylation of neurofilaments accompanies transmitter-related changes in rat septal neurons following transection of the fimbria-fornix. Brain Res 482:205–218.

Koliatsos VE, Price WL, Pardo CA, Price DL. 1994. Ventral root avulsion: an experimental model of death of adult motor neurons. J Comp Neurol 342:35–44.

Kong J, Xu Z. 1999. Peripheral axotomy slows motoneuron degeneration in a transgenic mouse line expressing mutant SOD1 G93A. J Comp Neurol 412:373–380.

Lowrie MB, Vrbová G. 1992. Dependence of postnatal motoneurones on their targets: review and hypothesis. Trend Neurosci 15:80–84.

Mariotti R, Cristino L, Bressan C, Boscolo B, Bentivoglio M. 2002. Altered reaction of facial motoneurons to axonal damage in the presymptomatic phase of a murine model of familial amyotrophic lateral sclerosis. Neuroscience 115:331–335.

Martin LJ, Kaiser A, Price AC. 1999. Motor neuron degeneration after nerve avulsion in adult evolves with oxidative stress and is apoptosis. J Neurobiol 40:185–201.

Moran LB, Graeber MB. 2004. The facial nerve axotomy model. Brain Res Rev 44:154–178.

Moreno S, Nardacci R, Ceru MP. 1997. Regional and ultrastructural immunolocalization of copper-zinc superoxide dismutase in rat central nervous system. J Histochem Cytochem 45:1611–1633.

Nagai M, Aoki M, Miyoshi I, Kato M, Pasinelli P, Kasai N, Brown RH Jr, Itoyama Y. 2001. Rats expressing human cytosolic copper-zinc superoxide dismutase transgenes with amyotrophic lateral sclerosis: associated mutations develop motor neuron disease. J Neurosci 21:9246–9254.

Nakagomi S, Suzuki Y, Namikawa K, Kiryu-Seo S, Kiyama H. 2003. Expression of the activating transcription factor 3 prevents c-Jun N-terminal kinase-induced neuronal death by promoting heat shock protein 27 expression and Akt activation. J Neurosci 23:5187–5196.

Okado-Matsumoto A, Fridovich I. 2002. Amyotrophic lateral sclerosis: a proposed mechanism. Proc Natl Acad Sci U S A 99:9010–9014.

Pardo CA, Xu Z, Borchelt DR, Price DL, Sisodia SS, Cleveland DW. 1995. Superoxide dismutase is an abundant component in cell bodies, dendrites, and axons of motor neurons and in a subset of other neurons. Proc Natl Acad Sci U S A 92:954–958.

Pearson AG, Gray CW, Pearson JF, Greenwood JM, During MJ, Dragunow M. 2003. ATF3 enhances c-Jun-mediated neurite sprouting. Brain Res Mol Brain Res 120:38–45.

Raivich G, Bohatschek M, Da Costa C, Iwata O, Galiano M, Hristova M, Nateri AS, Makwana M, Riera-Sans L, Wolfer DP, Lipp HP, Aguzzi A, Wagner EF, Behrens A. 2004. The AP-1 transcription factor c-Jun is required for efficient axonal regeneration. Neuron 43:57–67.

Rosenfeld J, Cook S, James R. 1997. Expression of superoxide dismutase following axotomy. Exp Neurol 147:37–47.

Sakamoto T, Watabe K, Ohashi T, Kawazoe Y, Oyanagi K, Inoue K, Eto Y. 2000. Adenoviral vector-mediated GDNF gene transfer prevents death of adult facial motoneurons. Neuroreport 11:1857–1860.

Sakamoto T, Kawazoe Y, Shen J-S, Takeda Y, Arakawa Y, Ogawa J, Oyanagi K, Ohashi T, Watanabe K, Inoue K, Eto Y, Watabe K. 2003a. Adenoviral gene transfer of GDNF, BDNF and TGFβ2, but not CNTF, cardiotrophin-1 or IGF1, protects injured adult motoneurons after facial nerve avulsion. J Neurosci Res 72:54–64.

Sakamoto T, Kawazoe Y, Uchida Y, Hozumi I, Inuzuka T, Watabe K. 2003b. Growth inhibitory factor prevents degeneration of injured adult rat motoneurons. Neuroreport 14:2147–2151.

Søreide AJ. 1981. Variations in the axon reaction after different types of nerve lesion. Acta Anat 110:173–188.

Tobisawa S, Hozumi Y, Arawaka S, Koyama S, Wada M, Nagai M, Aoki M, Itoyama Y, Goto K, Kato T. 2003. Mutant SOD1 linked to familial amyotrophic lateral sclerosis, but not wild-type SOD1, induces ER stress in COS7 cells and transgenic mice. Biochem Biophys Res Commun 303:496–503.

Tsujino H, Kondo E, Fukuoka T, Dai Y, Tokunaga A, Miki K, Yonenobu K, Ochi T, Noguchi K. 2000. Activating transcription factor 3 (ATF3) induction by axotomy in sensory and motoneurons: a novel neuronal marker of nerve injury. Mol Cell Neurosci 15:170–182.

Watabe K, Ohashi T, Sakamoto T, Kawazoe Y, Takeshima T, Oyanagi K, Inoue K, Eto Y, Kim SU. 2000. Rescue of lesioned adult rat spinal motoneurons by adenoviral gene transfer of glial cell line-derived neurotrophic factor. J Neurosci Res 60:511–519.

Wu W. 1993. Expression of nitric-oxide synthase (NOS) in injured CNS neurons as shown by NADPH diaphorase histochemistry. Exp Neurol 120:153–159.

Yoneda T, Inagaki S, Hayashi Y, Nomura T, Takagi H. 1992. Differential regulation of manganese and copper/zinc superoxide dismutases by the facial nerve transection. Brain Res 582:342–345.

Yu WHA. 2002. Spatial and temporal correlation of nitric oxide synthase expression with CuZn-superoxide dismutase reduction in motor neurons following axotomy. Ann N Y Acad Sci 962:111–121.

REGULAR PAPER

Shinsuke Kato · Masako Kato · Yasuko Abe
Tomohiro Matsumura · Takeshi Nishino · Masashi Aoki
Yasuto Itoyama · Kohtaro Asayama · Akira Awaya
Asao Hirano · Eisaku Ohama

Redox system expression in the motor neurons in amyotrophic lateral sclerosis (ALS): immunohistochemical studies on sporadic ALS, superoxide dismutase 1 (SOD1)-mutated familial ALS, and SOD1-mutated ALS animal models

Abstract Peroxiredoxin-ll (Prxll) and glutathione peroxidase-1 (GPxl) are regulators of the redox system that is one of the most crucial supporting systems in neurons. This system is an antioxidant enzyme defense system and is synchronously linked to other important cell supporting systems. To clarify the common self-survival mechanism of the residual motor neurons affected by amyotrophic lateral sclerosis (ALS), we examined motor neurons from 40 patients with sporadic ALS (SALS) and 5 patients with superoxide dismutase 1 (SOD1)-mutated familial ALS (FALS) from two different families (frameshift 126 mutation and A4 V) as well as four different strains of the SOD1-mutated ALS models (H46R/G93A rats and G1H/G1L-G93A mice). We investigated the immunohistochemical expression of Prxll/GPxl in motor neurons from the viewpoint of the redox system. In normal subjects, Prxll/GPxl immunoreactivity in the anterior horns of the normal spinal cords of humans, rats and mice was primarily identified in the neurons: cytoplasmic staining was observed in almost all of the motor neurons. Histologically, the number of spinal motor neurons in ALS decreased with disease progression. Immunohistochemically, the number of neurons negative for Prxll/GPxl increased with ALS disease progression. Some residual motor neurons coexpressing Prxll/GPxl were, however, observed throughout the clinical courses in some cases of SALS patients, SOD1-mutated FALS patients, and ALS animal models. In particular, motor neurons overexpressing Prxll/GPxl, i.e., neurons showing redox system up-regulation, were commonly evident during the clinical courses in ALS. For patients with SALS, motor neurons overexpressing Prxll/GPxl were present mainly within approximately 3 years after disease onset, and these overexpressing neurons thereafter decreased in number dramatically as the disease progressed. For SOD1-mutated FALS patients, like in SALS patients, certain residual motor neurons without inclusions also overexpressed Prxll/GPxl in the short-term-surviving FALS patients. In the ALS animal models, as in the human diseases, certain residual motor neurons showed overexpression of Prxll/GPxl during their clinical courses. At the terminal stage of ALS, however, a disruption of this common Prxll/GPxl-overexpression mechanism in neurons was observed. These findings lead us to the conclusion that the residual ALS neurons showing redox system up-regulation would be less susceptible to ALS stress and protect themselves from ALS neuronal death, whereas the breakdown of this redox system at the advanced disease stage accelerates neuronal degeneration and/or the process of neuronal death.

S. Kato (✉) · E. Ohama
Department of Neuropathology, Institute of Neurological
Sciences, Faculty of Medicine, Tottori University,
Nishi-cho 36-1, 683-8504 Yonago, Japan
E-mail: kato@grape.med.tottori-u.ac.jp
Tel.: +81-859-348034
Fax: +81-859-348289

M. Kato
Division of Pathology, Tottori University Hospital,
Yonago, Japan

Y. Abe · T. Matsumura · T. Nishino
Department of Biochemistry and Molecular Biology,
Nippon Medical School, Tokyo, Japan

M. Aoki · Y. Itoyama
Department of Neuroscience, Division of Neurology,
Tohoku University Graduate School of Medicine, Sendai, Japan

K. Asayama
Department of Pediatrics, University of Occupational and
Environmental Health, Kitakyushu, Japan

A. Awaya
Japan Science and Technology Agency, Tachikawa, Japan

A. Hirano
Division of Neuropathology, Department of Pathology,
Montefiore Medical Center, Bronx, New York, USA

Introduction

Amyotrophic lateral sclerosis (ALS), first described by
Charcot and Joffroy in 1869 [11], is a fatal and age-
associated neurodegenerative disorder that primarily
involves both the upper and lower motor neurons [23].
This disease has been recognized as a distinct clinico-
pathological entity of unknown etiology for over
130 years.

During physiological processes and in response to
external stimuli such as ultraviolet radiation, cells pro-
duce reactive oxygen species (ROSs). To protect itself
from these potentially destructive ROSs, each cell of the
living organs has developed a sophisticated antioxidant
system. In such systems, there are two groups of the
enzymes: those constituting the first group convert
superoxide radicals into hydrogen peroxide (H_2O_2), and
those of the second convert H_2O_2 into harmless water
and oxygen. The neuronal cytoplasmic isoform of the
first enzyme group is superoxide dismutase 1 (SOD1)
[13]. In the second enzyme group, there are the perox-
iredoxin (Prx) and glutathione peroxidase (GPx) fami-
lies, as well as catalase localized within peroxisomes.
Unlike in SOD1 and catalase, enzymes of the Prx and
GPx families require secondary enzymes and cofactors
to function at high efficiency [7]. The enzymes of the Prx
and GPx families are considered to play important roles
in the direct control of the redox system. In general, the
redox system regulates versatile control mechanisms in
signal transduction and gene expression [35]. In mam-
malian cells, this redox signal transduction is synchro-
nously linked to important systems such as cellular
differentiation, immune response, growth control,
apoptosis, and tumor growth [4, 9, 19, 26, 31, 34]. In the
mammalian central nervous system (CNS), the members
of Prx and GPx families regulating the neuronal cyto-
plasmic redox system are Prxll and GPxl, which directly
control the redox system in neurons [6, 7, 8, 12, 17, 24,
27, 29, 30]. In the in vivo milieu where mutant SOD1
exists, Prxll/GPxl co-aggregates with SOD1 as neuronal
Lewy body-like hyaline inclusions (LBHIs): neuronal
LBHIs immunohistochemically positive for three pro-
teins of SOD1, Prxll and GPxl are observed in the mu-
tant SOD1-related familial ALS (FALS) patients and
transgenic rats expressing human SOD1 with H46R and
G93A mutations [24]. Although some motor neurons
with SOD1 gene mutation form inclusions that are po-
sitive for these three proteins, other SOD1-mutated
motor neurons progress to cell death without forming
the inclusions.

On the other hand, an essential histopathological
feature of ALS is loss of the large anterior horn cells
throughout the spinal cord, with the surviving motor
neurons of the spinal cord exhibiting shrinkage. Among
these residual large anterior horn cells, some appear to be
normal. These surviving motor neurons in ALS patients
are thought to possess some form of self-preservation
mechanism. To gain new insight into the survival
mechanism of these residual motor neurons, we focused
on the redox system. In the study presented here, we
performed immunohistochemical analyses of the spinal
cord, not only from FALS patients with SOD1 gene
mutations and SOD1-mutated ALS animal models, but
also from patients with sporadic ALS (SALS), and
analyzed the expression of Prxll/GPxl (redox system) in
the residual motor neurons.

Materials and methods

Autopsy specimens

Histochemical and immunohistochemical studies were
performed on archival, buffered 10% formalin-fixed,
paraffin-embedded spinal cord tissues obtained at au-
topsy from 40 SALS patients and 5 FALS patients,
who were members of two different families. The main
clinical characteristics of the SALS patients are sum-
marized in Fig. 2. The clinicopathological characteris-
tics of the FALS patients are summarized in Table 1
and have been reported previously [20, 21, 25, 28, 33,
36, 38]. SOD1 analysis revealed that the members of
the Japanese Oki family had a two-base pair deletion at
codon 126 (frameshift 126 mutation) [20] and that the
members of the American C family had an Ala to Val
substitution at codon 4 (A4V) [36]. As controls for
human samples, we examined autopsy specimens of the
spinal cord from 20 neurologically and neuropatho-

Table 1 Characteristics of five FALS cases (*FALS* familial amyo-
trophic lateral sclerosis, *SOD* superoxide dismutase, *LBHI* Lewy
body-like hyaline inclusion, *2-bp* two-base pair, *PCI* posterior
column involvement type, + detected, *ND* not determined, *As*
asphyxia, *IH* intraperitoneal hemorrhage, *RD* respiratory distress,
Pn pneumonia)

Case	Age	Sex	Cause of death	FALS duration	SOD1 mutation	FALS subtype	Neuronal LBHI
Japanese Oki family							
1	46	F	As	18 months	2-bp deletion (126)	PCI	+
2	65	M	IH	11 years	2-bp deletion (126)	PCI and degeneration of other systems	+
American C family							
3	39	M	RD	7 months	A4V	PCI	+
4	46	M	Pn	8 months	A4V	PCI	+
5	66	M	Pn	1 year	ND	PCI	+

logically normal individuals (11 males, 9 females; aged 37–75 years).

Animal models

Histochemical and immunohistochemical studies were also carried out on specimens from ALS animal models: transgenic rats and mice carrying the overexpressed human mutant SOD1 genes. The H46R rats used in this study were a transgenic line (H46R-4) in which the level of human SOD1 with the H46R mutation was 6 times the level of endogenous rat SOD1 [32]. The G93A rats were a transgenic line (G93A-39) in which the level of human SOD1 with the G93A mutation was 2.5 times the level of endogenous rat SOD1 [32]. The G93A mice used in this study represented two lines of transgenic mice carrying the overexpressed human G93A mutant SOD1 gene: high copy G93A mice [B6SJL-TgN(SOD1-G93A)1Gur, JR2726; G1H-G93A] and low copy G93A mice [B6SJL-TgN(SOD1-G93A)1Gur^{dl}, JR2300; G1L-G93A] (Jackson Laboratory, Bar Harbor, ME). The H46R rats were killed at 110 ($n=1$), 135 ($n=1$), 160 ($n=1$), 170 ($n=1$), and over 180 ($n=3$) days after birth. The G93A rats were killed at 70 ($n=1$), 90 ($n=1$), 110 ($n=1$), 130 ($n=1$), 150 ($n=1$), and over 180 ($n=3$) days after birth. The detailed clinical signs and pathological characteristics of the H46R and G93A rats have been demonstrated previously [32]. As rat controls, we investigated the spinal cord specimens of each of eight age-matched littermates of the H46R and G93A rats. The G1H-G93A mice were examined at 90 ($n=2$), 100 ($n=2$), 110 ($n=3$), and 120 ($n=3$) days of age. The G1L-G93A mice were examined at 90 ($n=1$), 100 ($n=1$), 120 ($n=1$), 150 ($n=1$), 180 ($n=1$), 190 ($n=1$), 215 ($n=1$), 230 ($n=1$), and over 250 ($n=2$) days of age. As mouse controls, we also examined the spinal cord specimens of each of ten age-matched littermates of the G1H-G93A and G1L-G93A mice. Rats and mice were anesthetized with sodium pentobarbital (0.1 ml/100 g body weight). After perfusion of the animals via the aorta with physiological saline at 37°C, they were fixed by perfusion with 4% paraformaldehyde in 0.1 M cacodylate buffer (pH 7.3). The spinal cords were removed and then postfixed in the same solution. This study was approved by the Institutional Animal Care and Use Committee of Tottori University (Permission no. 03-S-18).

Histochemistry and immunohistochemistry

After fixation, the specimens were embedded in paraffin, cut into 6-μm-thick sections and examined by light microscopy. Spinal cord sections were stained by the following histochemical methods: hematoxylin and eosin (HE), Klüver-Barrera, Holzer, phosphotungstic acid-hematoxylin, periodic acid-Schiff, alcian blue, Masson's trichrome, Mallory azan, and Gallyas-Braak stains.

Rat PrxII, which contained a 6-His-tagged sequence at the N-terminal region, was overexpressed using *Escherichia coli* strain BL21 (DE3) cells harboring the expression plasmid pET30a (Novagen, Darmstadt, Germany) -PrxII, according to the modified method by Hirotsu et al. [15]. The His-tagged PrxII induced with 0.1 mM isopropyl-β-D-thiogalactoside (IPTG) was purified by a Ni^{2+}-nitrilotriacetate column (Qiagen, Hilden, Germany) and then digested with enterokinase. Finally, the purified PrxII was passed through an Erapture Agarose column for removal of enterokinase (Novagen). The PrxII gene was prepared from a rat liver cDNA library (Takara Biomedicals, Otsu, Japan) by PCR using the primers, 5'-TTCCATGGCCTCCGG-CAACGCGCACAT-3' and 5'-TTGGATCCATCTCA-GTTGTGTTTGGAG-3'. Utilizing this purified recombinant rat PrxII protein (amino acids 1–198), we produced a rabbit polyclonal antibody against rat PrxII according to the method previously described by Kato et al. [24].

Representative paraffin sections were used for immunohistochemical assays. The following primary antibodies were used: a rabbit polyclonal antibody against rat PrxII (amino acids 1–198) [diluted 1:2,000 in 1% bovine serum albumin-containing phosphate-buffered saline (BSA-PBS), pH 7.4]; an affinity-purified rabbit antibody against a synthetic peptide corresponding to the C-terminal region of PrxII (amino acids 184–198; this amino acid sequence is homologous with those of the C-terminal regions of the human, rat or mouse PrxII.) (concentration: 1 μg/ml) [24]; a polyclonal antibody to GPx1 [diluted 1:2,000 in 1% BSA-PBS, pH 7.4] [3]; a polyclonal antibody to human SOD1 (diluted 1:10,000 in 1% BSA-PBS, pH 7.4) [2]; and a monoclonal antibody to human SOD1 (concentration: 3 μg/ml; MBL, Nagoya, Japan). Sections were deparaffinized, and endogenous peroxidase activity was quenched by incubation for 30 min with 0.3% H$_2$O$_2$. The sections were then washed in PBS. Normal sera homologous with the secondary antibodies were used as a blocking reagent. Tissue sections were incubated with the primary antibodies for 18 h at 4°C. PBS-exposed sections served as controls. As a further control, some sections were incubated with the polyclonal antibody against rat PrxII that had been preabsorbed with an excess amount of the recombinant rat PrxII protein. Bound antibodies were visualized by the avidin-biotin-immunoperoxidase complex (ABC) method using the appropriate Vectastain ABC kits (Vector Laboratories, Burlingame, CA) and 3,3'-diaminobenzidine tetrahydrochloride (DAB; Dako, Glostrup, Denmark) as chromogen.

Western blot analysis

This analysis was carried out on three fresh autopsy specimens from spinal cord cervical segments obtained from two SALS cases [2.5 years after onset (case 19 in Fig. 2: age 63 years) and 11 years 5 months after onset

(case 40 in Fig. 2: age 51 years)] and one normal indi-vidual (age 68 years). In brief, specimens were homoge-nized in Laemmli sample buffer (Bio-Rad, Hercules, CA) containing 2% sodium dodecyl sulfate (SDS), 25% glycerol, 10% 2-mercaptoethanol, 0.01% bromophenol blue, and 62.5 mM TRIS-HCl (pH 6.8). The samples were heated at 100°C for 5 min. Soluble protein extracts (20 µg) from the samples were separated on SDS-poly-acrylamide gels (4–20% gradient, Bio-Rad) and trans-ferred by electroblotting to Immobilon PVDF (Millipore, Bedford, MA). After blocking with 5% nonfat milk for 30 min at room temperature, the blots were incubated

overnight at 4°C with the antibodies against PrxII and GPxl. Binding to Prxll and GPxl was visualized with the Vectastain ABC Kit and DAB. Appropriate molecular weight markers (Bio-Rad) were included in each run.

Results

Histopathology

An important histopathological finding in the spinal cord in SALS was loss of motor neurons throughout the

Fig. 1 Detection of PrxII and GPxI in serial sections of the normal anterior horn cells of the spinal cord in humans (A–C) and rats (D–F). **A, D** HE staining. **B, E** Immunoreactive for PrxII: immunostaining with the antibody against synthetic peptide corresponding to the C-terminal region of Prxll (**B**) and immunostaining with the antibody to rat PrxII (**E**). Immunoreactivity is identified in most of the anterior horn cells. **C, F** Immunostaining for GPxl. Almost all of the anterior horn cells in the spinal cord coexpress both PrxII (**B, E**) and GPxl (**C, F**) in comparison with HE-stained serial sections (**A, D**), although their staining intensities in neurons vary. **B, C, E, F** No counterstaining. (*HE* hematoxylin and eosin, *PrxII* peroxiredoxin-II, *GPxI* glutathione peroxidase-I). *Bars* **A** (also for **B, C**), **D** (also for **E, F**) 100 µm
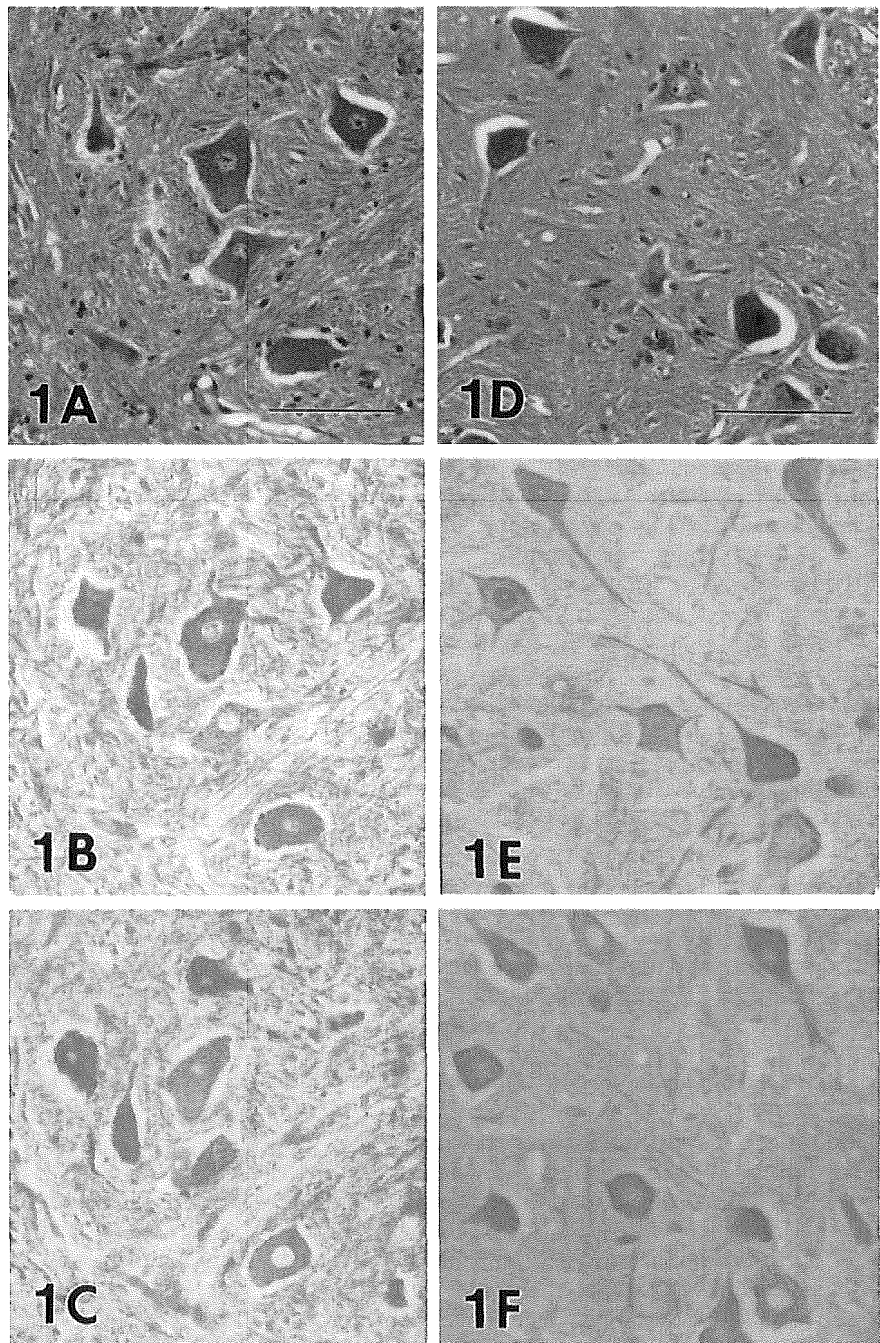
course of the disease. In the specimens we examined, neuronal loss was most easily recognized in the cervical and lumbar enlargements. The surviving motor neurons showed shrinkage, and lipofuscin granule-filled neurons stood out. Among the residual motor neurons, some appeared to be normal. Bunina bodies were observed in the residual motor neurons. The number of motor neurons decreased with SALS disease progression. Reactive astrocytosis and gliosis were also observed in the affected areas. In the affected antero-lateral columns that were most pronounced in the crossed and uncrossed corticospinal tracts, there was a loss of large myelinated fibers in association with variable degrees of astrocytic gliosis. Fiber destruction was associated with the appearance of lipid-laden macrophages. Analysis of the essential changes in the five cases of SOD1-mutated FALS revealed a subtype of FALS with posterior column involvement (PCI). This subtype is characterized by degeneration of the middle root zones of the posterior column, Clarke nuclei, and the posterior spinocerebellar tracts, in addition to spinal cord motor neuron lesions. A patient who had survived for a long period, with a clinical course of 11 years (case 2 in Table 1), showed multi-system degeneration in addition to the features of FALS with PCI. Neuronal LBHIs were present in all five FALS cases with SOD1 gene mutations. The spinal cords of normal human individuals did not exhibit any distinct histopathological alterations.
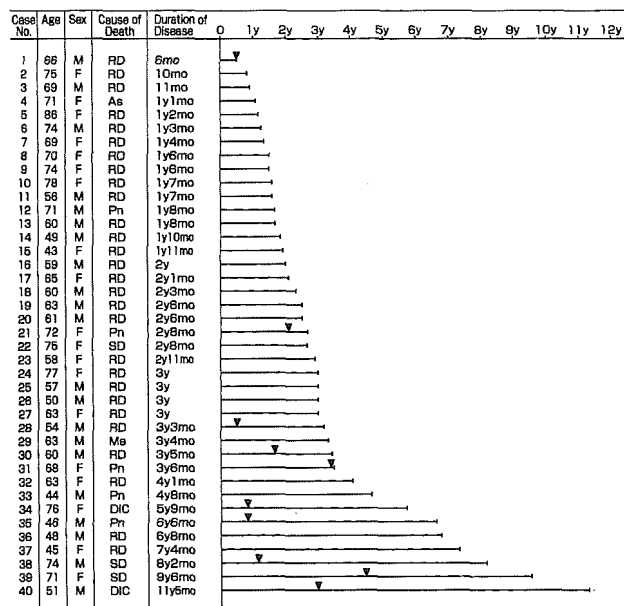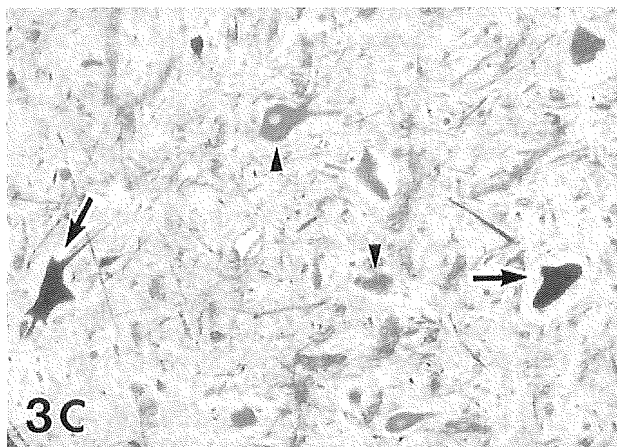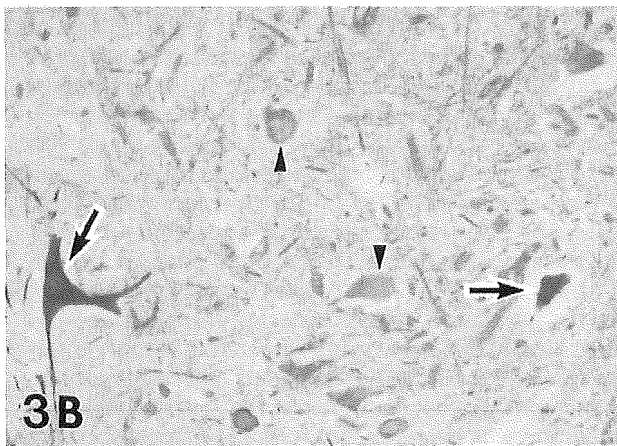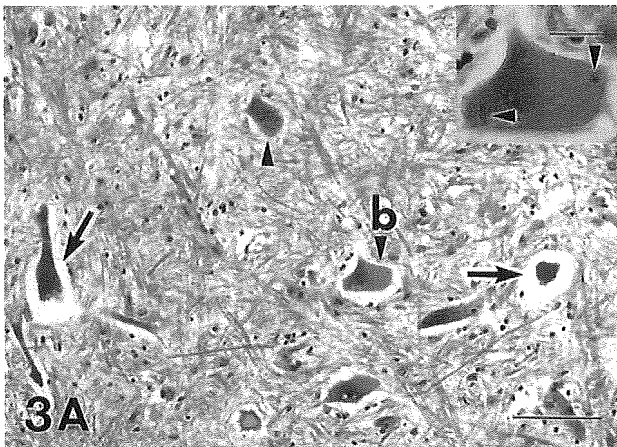

Fig. 2 Characteristics of 40 SALS cases, including patient's age, sex, cause of death, and duration of disease. The *horizontal lines* each show the duration of disease. *Arrowheads* indicate the time point at which the patients were placed on respirators (*ALS* amyotrophic lateral sclerosis, *SALS* sporadic ALS, *RD* respiratory distress, *As* asphyxia, *Pn* pneumonia, *SD* sudden death, *Me* melena, *DIC* disseminated intravascular coagulation, *y* years, *mo* months)

The clinical courses and histopathological findings of H46R and G93A transgenic rats have been reported previously by Nagai et al. [32]. As expected, the H46R rats developed motor deficits at approximately 145 days of age, and G93A rats showed the clinical signs at around 125 days of age. When we focused on the anterior horn cells, the number of the anterior horn cells of the H46R rat at 110 days of age was not significantly decreased as compared with that of the age-matched littermate. There were slightly decreased numbers of anterior horn cells with inclusions in the H46R rat at 135 days of age. At 160, 170 and over 180 days of age, the number of the anterior horn cells in the H46R rats was decreased markedly, and many inclusions including neuronal LBHIs were observed as inclusion pathology. For G93A rats, the number of the anterior horn cells at 70, 90 and 110 days of age was almost the same as that of their age-matched littermates, although at 90 and 110 days of age these rats showed vacuolation pathology including neuropil vacuoles. In G93A rats at 130, 150 and over 180 days of age, there was marked loss of the anterior horn cells, with both inclusion and vacuolation pathologies being involved. In the transgenic mice from the Jackson Laboratory, the clinical onset of the G1H-G93A mice was, as expected, about 100 days after birth, and that of G1L-G93A mice was approximately 185 days after birth. The number of the anterior horn cells of the G1H-G93A mice examined at 90 days after birth was not significantly decreased as compared with that of their age-matched littermates, whereas neuropil vacuolation was observed. The number of anterior horn cells of the G1H-G93A mice at 100 days of age was slightly decreased, and they had abundant vacuoles and a few inclusions. The G1H-G93A mice examined at 110 and 120 days of age revealed severe loss of the anterior horn cells and both inclusion and vacuolation pathologies. In the G1L-G93A mice examined at 90, 100, 120, 150 and 180 days after birth, the number of the anterior horn cells was not significantly changed compared to that of their age-matched littermates, although the G1L-G93A mice at 90, 100, 120, 150 and 180 days of age showed vacuolation pathology and, at 180 days of age, a few inclusions. In G1L-G93A mice at 190, 215, 230 and over 250 days of age, there were significant losses of anterior horn cells, with both inclusion and vacuolation pathologies being present. The spinal cords of the littermates of these animal models did not exhibit any distinct histopathological changes.

Immunohistochemistry

In the present study, we produced a rabbit polyclonal antibody against rat PrxII (amino acids 1–198), in addition to the affinity-purified rabbit antibody against a synthetic peptide corresponding to the C-terminal region of PrxII previously reported by Kato et al. [24]. This newly produced rabbit polyclonal antibody against rat PrxII was successfully applied to stain paraffin sections

Fig. 3 Serial sections of the spinal anterior horn cells in a patient with SALS after a clinical course of 2.5 years (case 19 in Fig. 2). **A** Light microscopic preparation stained with HE. *Top right inset* shows the higher magnification of a neuron (indicated by *arrowhead* with **b** in **A**), in which Bunina bodies (*arrowheads* in *top right inset*) are observed. **B** PrxII immunoreactivity of the section consecutive to that shown in **A**. **C** GPxI immunoreactivity of the section consecutive to that shown in **B**. Residual neurons overexpressing both PrxII and GPxI are evident (*arrows*). The staining pattern is diffuse in the cytoplasm and dendrites. Other neurons are either faintly stained by both antibodies, or unstained (*arrowheads*). Observation of only the HE-stained section in **A** reveals no difference between the neurons overexpressing PrxII/GPxI and those almost negative for PrxII/GPxI. No correlation is demonstrated between PrxII/GPxI expression and the presence of Bunina bodies. **B**, **C** No counterstaining. *Bar* **A** (also for **B**, **C**) 100 μm, *top right inset* in **A** 20 μm

pretreated with an excess amount of the recombinant rat PrxII protein (amino acids 1–198) produced no staining in any of the sections.

As expected [24], almost all of the normal anterior horn cells in the spinal cords of humans, rats and mice coexpressed both PrxII and GPxI (Fig. 1), although their staining intensities in positively stained neurons varied. With respect to the intracellular localization of PrxII using the two anti-PrxII antibodies, immunostaining of the neuronal cytoplasm and proximal dendrites was specifically observed (Fig. 1B, E). In addition, the nuclei of some neurons were immunostained, albeit the staining intensity varied (Fig. 1E). GPxI immunostaining showed a cytoplasmic staining pattern, with the cell bodies and proximal dendrites being essentially identified (Fig. 1C, F), but no intranuclear staining was observed (Fig. 1C, F).

In SALS patients, some residual neurons expressed both PrxII and GPxI strongly within about 3 years after disease onset (cases 1–27 in Fig. 2). Other neurons were either faintly stained by both antibodies or unstained. Around 2–3 years after disease onset in SALS patients (cases 16–27 in Fig. 2), the intensity of PrxII and GPxI immunoreactivities peaked in some residual neurons that were positive for both proteins (Fig. 3). In SALS patients with a clinical course of over 3 years (cases 28–40 in Fig. 2), the number of residual neurons decreased strikingly, and respiratory assistance became essential for most patients. The residual neurons intensely expressing both PrxII and GPxI decreased with disease progression, while the number of residual neurons negative for both proteins increased dramatically (Fig. 4). At 11 years 5 months after disease onset (case 40 in Fig. 2), most of the neurons were atrophic and immunonegative for both PrxII and GPxI. However, even in this long-surviving patient, a few residual neurons expressing both PrxII and GPxI were observed (Fig. 5). Thus, residual motor neurons positive for both PrxII and GPxI were always evident throughout the disease course in every SALS patient, although after approximately 3 years of disease their number decreased dramatically. Observation of only the HE-stained sections revealed no

from rats (Fig. 1E). Additionally, we were able to use this rabbit polyclonal antibody against rat PrxII to stain paraffin sections from humans and mice. Both anti-PrxII antibodies had the same ability to immunostain paraffin sections from humans, rats and mice, as well as in immunoblotting of tissue homogenate of the human spinal cord. When control and representative paraffin sections were incubated with PBS alone (i.e., no primary antibody), no staining was detected. Incubation of sections with anti-rat PrxII antibody that had been

Fig. 4 Serial sections of the
spinal anterior horn cells in a
patient with SALS after a
clinical course of 4 years
8 months (case 33). A In the HE
preparation, residual motor
neurons appear to be atrophic.
There is no distinction among
these atrophic neurons when
observed in the HE preparation
alone. B Immunostaining for
Prxll. The number of residual
neurons overexpressing Prxll
(*arrow*) is reduced in
comparison with that in the
SALS patient after a clinical
course of 2.5 years (Fig. 3). The
number of Prxll-negative
neurons is increased
(*arrowheads*).
C Immunostaining for GPxl.
Similarly to the Prxll
immunostaining, the number of
GPxl-overexpressing neurons is
diminished (*arrow*). In contrast,
the number of GPxl-
immunonegative neurons is
increased (*arrowheads*). B, C No
counterstaining. Bar A (also for
B, C) 100 μm
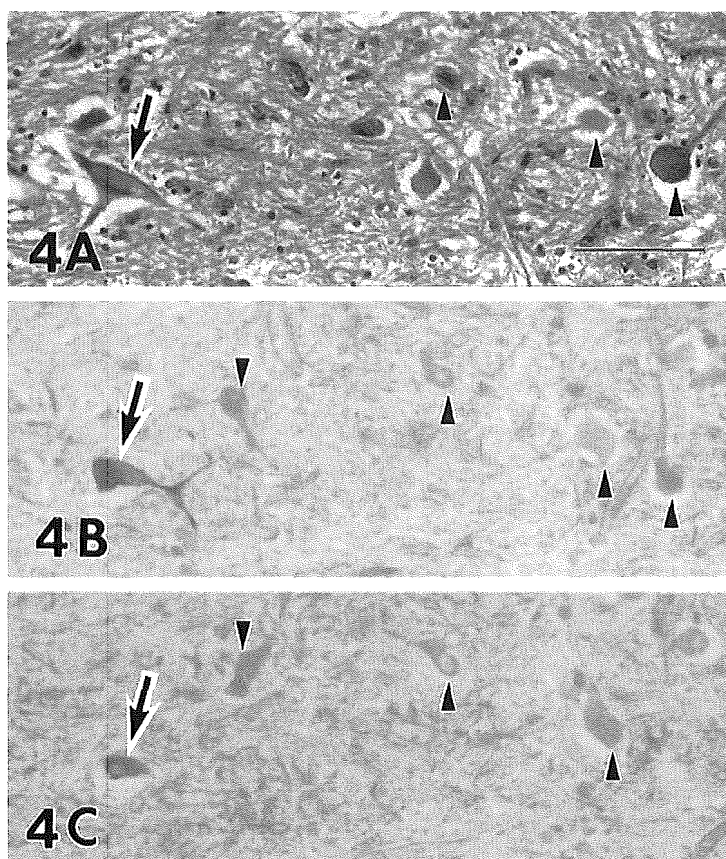
difference between the neurons positive for Prxll and GPxl and those negative for both proteins (Figs. 3, 4, 5).

In the five FALS patients with SOD1 mutations, as reported previously [24], neuronal LBHIs in the anterior horn cells showed co-aggregation of Prxll/GPxl with SOD1. Although some SOD1-mutated anterior horn cells in these patients formed neuronal LBHIs, others did not. When we focused on these residual anterior horn cells without inclusions, the stainability and intensity of Prxll and GPxl staining in the residual cells without inclusions in the five FALS patients with SOD1 gene mutations were identical to those of the SALS patients. The numbers of residual anterior horn cells in one member of the Japanese Oki family (case 1, frame-shift 126 mutation in SOD1 gene) and three members of the American C family (cases 3–5, A4V substitution in the SOD1 gene), observed within 2 years of the disease onset, were similar, although the loss of the anterior horn cells in the FALS patients was generally more severe in contrast to that seen in the SALS patients with the same disease duration. As in the SALS patients within about 3 years of disease onset, some of the residual anterior horn cells with no LBHIs overexpressed Prxll/GPxl in the four short-term-surviving FALS patients from the two different families and divergent SOD1 gene mutations. In a long-term surviving patient (case 2) with a clinical course of over 10 years, there

were a few residual neurons, and most were immuno-negative for Prxll/GPxl. However, rare residual neurons expressing Prxll/GPxl were still evident. The findings for the long-term-surviving FALS patient with SOD1 mutation were the same as those of the long-term-surviving SALS patients.

In the ALS animal models with human mutant SOD1, the inclusions exhibited co-aggregation of Prxll/GPxl with SOD1 as reported previously [24]. Notice-ably, the Prxll/GPxl-immunoreactive findings in the rat (H46R and G93A rats) and mouse (G1H-G93A and G1L-G93A mice) models were essentially the same throughout the disease course for each ALS animal model. In the preclinical stage, the Prxll/GPxl immu-nostainability and immunointensity of the anterior horn cells were identical to those in the anterior horn cells of the normal littermates. Although the number of the anterior horn cells in the ALS animal models was de-creased after the clinical onset of disease, some of these residual anterior horn cells showed overexpression of Prxll/GPxl, i.e., up-regulation of the redox system. In particular, this redox system up-regulation in the resid-ual motor neurons was prominent at 160 days of age in H46R rats (Fig. 6A, B), at 150 days of age in G93A rats, at 110 days of age in G1H-G93A mice (Fig. 7) and at 215 days of age in G1L-G93A mice. At the end stage of disease in the four different ALS animal models,
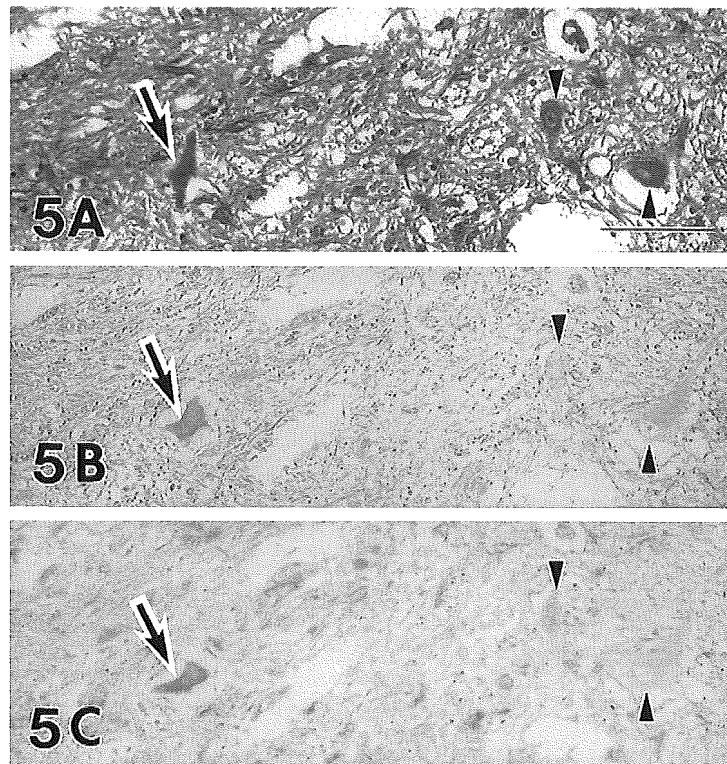
Fig. 5 Serial sections of the spinal anterior horn cells in a patient with SALS after a clinical course of 11 years 5 months (case 40). **A** Light microscopic preparation stained with HE. Small and atrophic motor neurons are seen. **B** PrxII immunoreactivity of the section consecutive to that shown in **A**. Although the residual neuron (*arrow*) appears to be atrophic in the HE preparation, this residual neuron expresses PrxII. **C** GPxI immunoreactivity of the section consecutive to that shown in **B**. The residual neuron that appears to be atrophic in the HE preparation is stained by the anti-GPxI antibody (*arrow*). Although there is no neuron overexpressing PrxII/GPxI, a neuron expressing PrxII/GPxI can be observed (*arrow*). By marked contrast, the number of neurons negative for PrxII/GPxI is increased (*arrowheads*). Observation of the HE-stained section in **A** shows no difference between the atrophic neuron positive for PrxII/GPxI (*arrow*) and the atrophic neurons negative for both proteins (*arrowheads*). **B, C** No counterstaining. *Bar* **A** (also for **B, C**) 100 μm

however, almost all of the residual motor neurons were negative for PrxII/GPxI, in marked contrast to the inclusions positive for PrxII/GPxI (Fig. 6C, D). As seen for the human specimens, no difference between the neurons positive for PrxII/GPxI and those negative for both proteins were observed the HE-stained sections for these animal models (Fig. 7).

Western blot analysis

When the tissue homogenate of each fresh cervical segment of the human spinal cord was examined by immunoblotting for PrxII, a single band corresponding to approximately 23 kDa was observed, i.e., with the same mobility as human PrxII (Fig. 8A). Immunoblotting showed that the intensity of PrxII immunoreactivity

in the SALS patient with a clinical course of 2.5 years (case 19 in Fig. 2) appeared to be almost identical to that in a normal subject. In the SALS patient with a clinical course of 11 years 5 months (case 40 in Fig. 2), PrxII expression was less than that in the normal subject. This observation supported the results of PrxII immunohistochemistry. Immunoblotting for GPxI revealed a single band corresponding to about 22 kDa in two SALS cases and a normal subject (Fig. 8B). This molecular mass was compatible with that of human GPxI. In the SALS case at 2.5 years after disease onset (case 19 in Fig. 2), GPxI was expressed with almost the same intensity as that in the normal subject. However, the level of GPxI expression in the SALS case at 11 years 5 months after onset (case 40 in Fig. 2) decreased below that in the normal subject. This finding reflected the GPxI immunohistochemistry results.

Discussion

PrxII is a novel organ-specific anti-oxidative enzyme that is mainly expressed in mammalian brain [24, 29]. It is a member of the Prx family, the members of which directly regulate the redox system [6, 7, 8, 17, 29]. PrxII is a homodimeric protein composed of two subunits, each with a molecular mass of approximately 23 kDa [15, 16]. Like PrxII, GPxI, one of the major cytosolic isoforms of the GPxI family, also directly controls the redox system [12, 27, 30]. GPxI is a homotetramer consisting of approximately 22-kDa subunits [3]. This is consistent with the results of Western blot analyses, where use of

Fig. 6 Expression of PrxII and GPxl detected by immunohistochemistry in the spinal anterior horn in the transgenic rats expressing human SOD1 with an H46R mutation. **A, B** Serial sections of spinal anterior horn cells at 160 days of age in H46R rat immunostained with antibodies against PrxII (**A**) and GPxl (**B**). Residual neurons overexpressing PrxII/GPxl, i.e., showing redox system up-regulation, are observed (*arrows*). An inclusion (*arrowhead* with *in*) in the neuropil is intensely positive for PrxII/GPxl. The other neurons are either faintly stained by both antibodies, or unstained (*arrowheads*). **C, D** Serial sections of spinal anterior horn cells at over 180 days of age in H46R rat immunostained with antibodies against PrxII (**C**) and GPxl (**D**). Round and sausage-like LBHIs are strongly positive for PrxII/GPxl (*arrows*). By marked contrast, the number of neurons negative for PrxII/GPxl is increased (*arrowheads*). **A—D** No counterstaining (*SOD* superoxide dismutase, *LBHI* Lewy body-like hyaline inclusion). *Bar* **A** (also for **B**) 50 μm, **C** (also for **D**) 30 μm
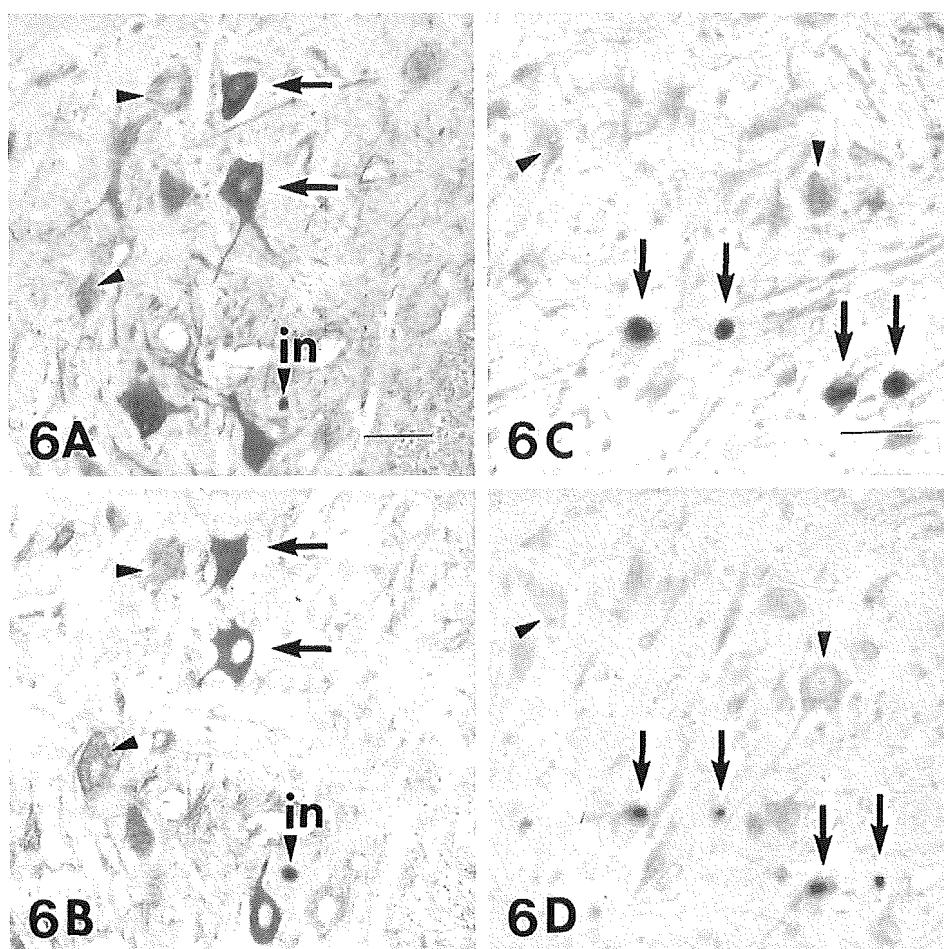
the normal human tissue homogenate yielded a single band of approximately 23 kDa with the two anti-PrxII antibodies and a single band of about 22 kDa with the anti-GPxl antibody.

As expected [24], PrxII/GPxl immunoreactivity in anterior horns of the normal spinal cords of humans, rats and mice was primarily identified in the neurons: cytoplasmic staining was observed in almost all of the anterior horn cells. Intranuclear localization in some neurons was also observed with PrxII immunostaining using the two anti-PrxII antibodies, as previously reported [24]. Considering that endogenous PrxII and GPxl within the neuronal cytoplasm are regulators of the redox system, our finding that almost all of the normal spinal motor neurons coexpressed PrxII/GPxl confirms that these motor neurons maintain themselves utilizing the intracellular PrxII/GPxl system, that is, the redox system.

Corroborating previous findings [24], neuronal LBHIs positive for SOD1, PrxII, and GPxl were observed in both the SOD1-mutated FALS patients and the four transgenic ALS animal models expressing human mutant SOD1. A breakdown of the redox system was seen in the SOD1-mutated motor neurons contain-

ing inclusions. It is possible that the intra-inclusional co-aggregation of PrxII/GPxl with SOD1, or the sequestration of PrxII/GPxl with SOD1 into the inclusions causes the intracytoplasmic reduction of PrxII/GPxl, thereby reducing the availability of the redox system [24]. Although inclusions were seen in some motor neurons with the SOD1 gene mutation, other SOD1-mutated motor neurons progressed to the cell death without forming the inclusions.

An interesting feature was the presence of certain residual motor neurons coexpressing PrxII/GPxl throughout the ALS disease course in SALS patients and among SOD1-mutated motor neurons without inclusions. A particularly striking finding was that motor neurons overexpressing PrxII/GPxl, i.e., with redox system up-regulation, were commonly evident during the clinical courses in the divergent disease subtypes: SALS patients, SOD1-mutated FALS patients, and ALS animal models expressing human mutant SOD1.

For the SALS patients, although the number of the residual SALS motor neurons decreased with the progression of the clinical disease, some motor neurons overexpressing PrxII/GPxl were present usually up to approximately 3 years after the onset, particularly in the
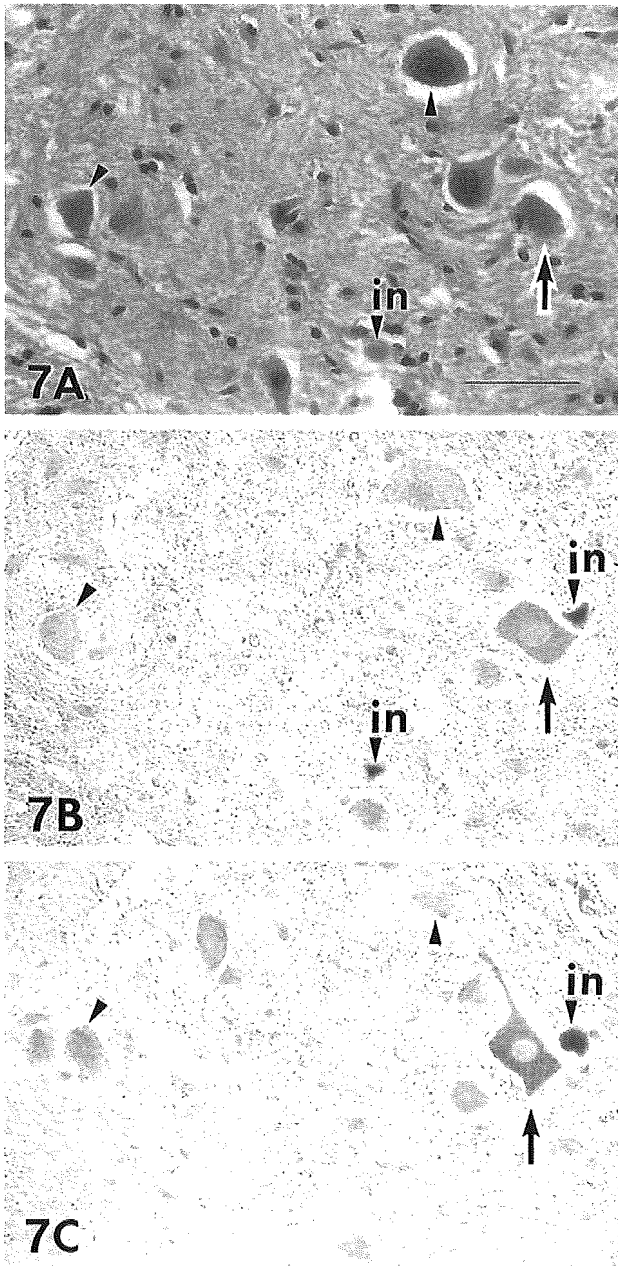
patients with no respiratory assistance. Thereafter, the number of these overexpressing motor neurons decreased dramatically as disease progressed. The immunohisto-chemical features are consistent with the Western blot findings that the levels of the Prxll/GPxl in the SALS patient after a clinical course of 2.5 years were almost the same levels as in normal cases in spite of loss of the motor neurons, whereas the levels decreased in the SALS patient after a clinical course of 11 years 5 months.

In the SOD1-mutated FALS patients, as in SALS patients, certain residual motor neurons without LBHIs also overexpressed Prxll/GPxl in the four short-term-surviving patients within 18 months after onset. In the ALS animal models, as in the human diseases, some residual motor neurons showed overexpression of Prxll/GPxl at 160 days of age in H46R rats, at 150 days of age in G93A rats, at 110 days of age in G1H-G93A mice and at 215 days of age in G1L-G93A mice. The presence of this common Prxll/GPxl-overexpression mechanism during the clinical course of ALS suggests that the redox system up-regulation represents one of the endogenous mechanisms that are activated by the ALS stress. At the terminal stage of ALS, however, disruption of this mechanism was observed. Although some residual ALS neurons coexpressed both proteins, while many others were negative, there was no apparent difference among these neurons on HE preparations.

In general, the redox system is one of the most crucial life supporting systems in living cells, serving as an antioxidant enzyme defense system that is synchro-nously linked to important physiological functions such as cellular differentiation, immune response, growth control, apoptosis, and tumor growth [4, 9, 19, 26, 31,
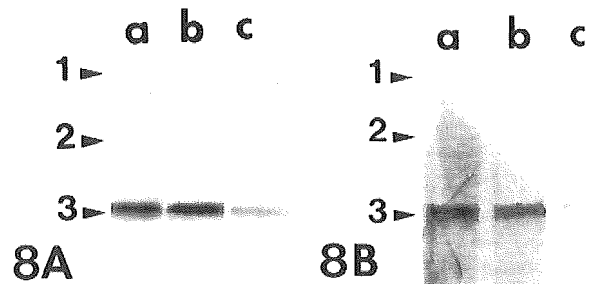

Fig. 7 Expression of Prxll and GPxl detected by immunohisto-chemistry in the spinal anterior horn in a G1H-G93A transgenic mouse carrying the highly overexpressed human G93A mutant SOD1 gene at 110 days of age. A Light microscopic preparation stained with HE. A round LBHI in the neuropil can be seen (arrowhead with in). B Prxll immunoreactivity of the section consecutive to that shown in A. C GPxl immunoreactivity of the section consecutive to that shown in B. Like in human ALS (Figs. 3, 4) and H46R rat (Fig. 6), a residual neuron overexpressing Prxll/GPxl, i.e., showing redox system up-regulation, can be observed (arrow). The other neurons are either faintly stained by both antibodies, or unstained (arrowheads), which indicates the breakdown of redox system. Round and sausage-like LBHIs in the neuropil are strongly positive for Prxll/GPxl (arrowhead with in). Observation of the HE-stained section in A reveals no difference between the neuron showing the redox system up-regulation (arrow) and the neurons exhibiting the redox system breakdown (arrowheads). B, C No counterstaining. Bar A (also for B, C) 50 μm

Fig. 8 Western blot analyses using the antibodies against Prxll (A) and GPxl (B). A 20-μg sample of the soluble protein extract from each sample was applied to each lane. Molecular mass markers: 1 ovalbumin (45 kDa); 2 carbonic anhydrase (31 kDa); 3 trypsin inhibitor (21.5 kDa). A Lane a: Normal control, lane b: an SALS patient with a clinical course of 2.5 years (case 19). lane c: an SALS patient with a clinical course of 11 years 5 months (case 40). A single band at approximately 23 kDa is observed in all samples. The intensity of Prxll immunoreactivity in lane b (ALS case 19) appears to be almost identical to that in lane a (normal). By contrast, Prxll expression in lane c (ALS case 40) appears to be lower than that in lane a (normal). B A single band of about 22 kDa is detected in each sample. Expression of GPxl in lane b (ALS case 19) shows almost the same intensity as that in lane a (normal). However, the level of GPxl expression in lane c (ALS case 40) is decreased below that seen in lane a (normal)

34]. Although we cannot exclude the possibility that the cells die as a result of redox stress itself, the residual ALS neurons expressing redox system up-regulation are thought to maintain their viability by protecting themselves from potentially destructive ROSs and by controlling the intraneuronal redox system [1, 5, 10, 14, 34, 39]. A similar up-regulation mechanism for hepatocyte growth factor (HGF, a novel neurotrophic factor) and its receptor (c-Met) also occurs in the SALS and SOD1-mutated FALS patients [22]. Considering that in the animal experiment, overexpression of HGF attenuates motor neuron death and prolongs the life span of G1L-G93A mice [37], motor neurons showing up-regulation of the HGF/c-Met cell-survival system, which is normally present in neurons, are thought to show enhanced cell survival in the presence of ALS stress in humans [22]. Although we cannot readily compare the neurotrophic factor with the redox system, our finding leads us to the conclusion that the residual ALS neurons showing redox system up-regulation would be less susceptible to ALS stress and can protect themselves from ALS neuronal death. Taken together with the fact that PrxII functions not only as a member of the redox system but also as a molecular chaperone [18], the residual ALS neurons overexpresing PrxII/GPxI might have developed to possess simultaneously both the enhanced antioxidant enzyme defense mechanism as a highly-evolved redox system, and the amplified sophisticated system for coping with misfolded proteins, such as mutant SOD1 or unknown pathogenetic proteins leading to SALS. Thus, residual ALS neurons overexpressing redox system-related enzymes could protect themselves from ALS stress. However, it is not thought possible for residual ALS neurons under long-term ALS stress to keep on inducing redox system-related enzymes. Therefore, as ALS progresses, the ability of residual neurons to up-regulate the redox system diminishes, and finally they become even unable to maintain the redox system itself. In other words, ALS neurons showing redox system up-regulation might show enhanced cell survival in the presence of ALS stress. In contrast, breakdown of the redox system in ALS motor neurons that are barely viable would result in cell death, and many residual motor neurons that are unable to coexpress PrxII/GPxI would ultimately become moribund.

Our data may lead to the development of a new therapy based on redox system up-regulation for the treatment of ALS, which for over 130 years has had an unknown etiology. It remains to be determined whether this redox system up-regulation is a direct or an indirect effect based on the pathogenesis of ALS itself, or whether this redox system up-regulation plays a primary or a secondary role in attenuating ALS-related neuronal death.

References

1. Andoh T, Chiueh CC, Chock PB (2003) Cyclic GMP-dependent protein kinase regulates the expression of thioredoxin and thioredoxin peroxidase-1 during hormesis in response to oxidative stress-induced apoptosis. J Biol Chem 278:885–890
2. Asayama K, Burr IM (1984) Joint purification of mangano and cuprozinc superoxide dismutases from a single source: a simplified method. Anal Biochem 136:336–339
3. Asayama K, Yokota S, Dobashi K, Hayashibe H, Kawaoi A, Nakazawa S (1994) Purification and immunoelectron microscopic localization of cellular glutathione peroxidase in rat hepatocytes: quantitative analysis by postembedding method. Histochemistry 102:213–219
4. Berggren MI, Husbeck B, Samulitis B, Baker AF, Gallegos A, Powis G (2001) Thioredoxin peroxidase-1 (peroxiredoxin-1) is increased in thioredoxin-1 transfected cells and results in enhanced protection against apoptosis caused by hydrogen peroxide but not by other agents including dexamethasone, etoposide, and doxorubicin. Arch Biochem Biophys 392:103–109
5. Biteau B, Labarre J, Toledano MB (2003) ATP-dependent reduction of cysteine-sulphinic acid by *S. cerevisiae* sulphiredoxin. Nature 425:980–984
6. Chae HZ, Kim IH, Kim K, Rhee SG (1993) Cloning, sequencing, and mutation of thiol-specific antioxidant gene of *Saccharomyces cerevisiae*. J Biol Chem 268:16815–16821
7. Chae HZ, Chung SJ, Rhee SG (1994) Thioredoxin-dependent peroxide reductase from yeast. J Biol Chem 269:27670–27678
8. Chae HZ, Robison K, Poole LB, Church G, Storz G, Rhee SG (1994) Cloning and sequencing of thiol-specific antioxidant from mammalian brain: alkyl hydroperoxide reductase and thiol-specific antioxidant define a large family of antioxidant enzymes. Proc Natl Acad Sci USA 91:7017–7021
9. Chang TS, Jeong W, Choi SY, Yu S, Kang SW, Rhee SG (2002) Regulation of peroxiredoxin I activity by cdc2-mediated phosphorylation. J Biol Chem 277:25370–25376
10. Chang TS, Jeong W, Woo HA, Lee SM, Park S, Rhee SG (2004) Characterization of mammalian sulfiredoxin and its reactivation of hyperoxidized peroxiredoxin through reduction of cysteine sulfinic acid in the active site to cysteine. J Biol Chem 279:50994–51001
11. Charcot JM, Joffroy A (1869) Deux cas d'atrophie musculaire progressive avec lésions de la substance grise et des faisceaux antéro-latéraux de la moelle épinière. Arch Physiol (Paris) 2:744–760
12. De Haan JB, Bladier C, Griffiths P, Kelner M, O'Shea RD, Cheung NS, Bronson RT, Silvestro MJ, Wild S, Zheng SS, Beart PM, Hertzog PJ, Kola I (1998) Mice with a homozygous null mutation for the most abundant glutathione peroxidase, Gpx1, show increased susceptibility to the oxidative stress-inducing agents paraquat and hydrogen peroxide. J Biol Chem 273:22528–22536
13. Fridovich I (1986) Superoxide dismutases. Adv Enzymol Relat Areas Mol Biol 58:61–97
14. Georgiou G, Masip L (2003) An overoxidation journey with a return ticket. Science 300:592–594
15. Hirotsu S, Abe Y, Nagahara N, Hori H, Nishino T, Okada K, Hakoshima T (1999) Crystallographic characterization of a stress-induced multifunctional protein, rat HBP-23. J Struct Biol 126:80–83
16. Hirotsu S, Abe Y, Okada K, Nagahara N, Hori H, Nishino T, Hakoshima T (1999) Crystal structure of a multifunctional 2-Cys peroxiredoxin heme-binding protein 23 kDa/proliferation-associated gene product. Proc Natl Acad Sci USA 96:12333–12338

17. Ichimiya S, Davis JG, O'Rourke DM, Katsumata M, Greene MI (1997) Murine thioredoxin peroxidase delays neuronal apoptosis and is expressed in areas of the brain most susceptible to hypoxic and ischemic injury. DNA Cell Biol 16:311–321

18. Jang HH, Lee KO, Chi YH, Jung BG, Park SK, Park JH, Lee JR, Lee SS, Moon JC, Yun JW, Choi YO, Kim WY, Kang JS, Cheong GW, Yun DJ, Rhee SG, Cho MJ, Lee SY (2004) Two enzymes in one; two yeast peroxiredoxins display oxidative stress-dependent switching from a peroxidase to a molecular chaperone function. Cell 117:625–635

19. Jin D-Y, Chae HZ, Rhee SG, Jeang K-T (1997) Regulatory role for a novel human thioredoxin peroxidase in NF-kappaB activation. J Biol Chem 272:30952–30961

20. Kato S, Shimoda M, Watanabe Y, Nakashima K, Takahashi K, Ohama E (1996) Familial amyotrophic lateral sclerosis with a two base pair deletion in superoxide dismutase 1 gene: multisystem degeneration with intracytoplasmic hyaline inclusions in astrocytes. J Neuropathol Exp Neurol 55:1089–1101

21. Kato S, Hayashi H, Nakashima K, Nanba E, Kato M, Hirano A, Nakano I, Asayama K, Ohama E (1997) Pathological characterization of astrocytic hyaline inclusions in familial amyotrophic lateral sclerosis. Am J Pathol 151:611–620

22. Kato S, Funakoshi H, Nakamura T, Kato M, Nakano I, Hirano A, Ohama E (2003) Expression of hepatocyte growth factor and c-Met in the anterior horn cells of the spinal cord in the patients with amyotrophic lateral sclerosis (ALS): immunohistochemical studies on sporadic ALS and familial ALS with superoxide dismutase 1 gene mutation. Acta Neuropathol 106:112–120

23. Kato S, Shaw P, Wood-Allum C, Leigh PN, Show C (2003) Amyotrophic lateral sclerosis. In: Dickson D (ed) Nerodegeneration: the molecular pathology of dementia and movement disorders. ISN Neuropath Press, Basel, pp 350–368

24. Kato S, Saeki Y, Aoki M, Nagai M, Ishigaki A, Itoyama Y, Kato M, Asayama K, Awaya A, Hirano A, Ohama E (2004) Histological evidence of redox system breakdown caused by superoxide dismutase 1 (SOD1) aggregation is common to SOD1-mutated motor neurons in humans and animal models. Acta Neuropathol 107:149–158

25. Kato T, Hirano A, Kurland LT (1987) Asymmetric involvement of the spinal cord involving both large and small anterior horn cells in a case of familial amyotrophic lateral sclerosis. Clin Neuropathol 6:67–70

26. Koo KH, Lee S, Jeong SY, Kim ET, Kim HJ, Kim K, Song K, Chae HZ (2002) Regulation of thioredoxin peroxidase activity by c-terminal truncation. Arch Biochem Biophys 397:312–318

27. Kosower NS, Kosower EM (1978) The glutathione status of cells. Int Rev Cytol 54:109–160

28. Kurland LT, Mulder DW (1955) Epidemiologic investigations of amyotrophic lateral sclerosis. II. Familial aggregations indicative of dominant inheritance. Neurology 5:182–196, 249–268

29. Matsumoto A, Okado A, Fujii T, Fujii J, Egashira M, Niikawa N, Taniguchi N (1999) Cloning of the peroxiredoxin gene family in rats and characterization of the fourth member. FEBS Lett 443:246–250

30. Meister A, Anderson ME (1983) Glutathione. Annu Rev Biochem 52:711–760

31. Mu ZM, Yin XY, Prochownik EV (2002) Pag, a putative tumor suppressor, interacts with the myc box II domain of c-myc and selectively alters its biological function and target gene expression. J Biol Chem 277:43175–43184

32. Nagai M, Aoki M, Miyoshi I, Kato M, Pasinelli P, Kasai N, Brown RH Jr, Itoyama Y (2001) Rats expressing human cytosolic copper-zinc superoxide dismutase transgenes with amyotrophic lateral sclerosis: associated mutations develop motor neuron disease. J Neurosci 21:9246–9254

33. Nakano I, Hirano A, Kurland LT, Mulder DW, Holley PW, Saccomanno G (1984) Familial amyotrophic lateral sclerosis. Neuropathology of two brothers in American "C" family. Neurol Med (Tokyo) 20:458–471

34. Neumann CA, Krause DS, Carman CV, Das S, Dubey DP, Abraham JL, Bronson RT, Fujiwara Y, Orkin SH, Van Etten RA (2003) Essential role for the peroxiredoxin prdx1 in erythrocyte antioxidant defence and tumour suppression. Nature 424:561–565

35. Sen CK, Packer L (1996) Antioxidant and redox regulation of gene transcription. FASEB J 10:709–720

36. Shibata N, Hirano A, Kobayashi M, Siddique T, Deng HX, Hung WY, Kato T, Asayama K (1996) Intense superoxide dismutase-1 immunoreactivity in intracytoplasmic hyaline inclusions of familial amyotrophic lateral sclerosis with posterior column involvement. J Neuropathol Exp Neurol 55:481–490

37. Sun W, Funakoshi H, Nakamura T (2002) Overexpression of HGF retards disease progression and prolongs life span in a transgenic mouse model of ALS. J Neurosci 22:6537–6548

38. Takahashi K, Nakamura H, Okada E (1972) Hereditary amyotrophic lateral sclerosis. Histochemical and electron microscopic study of hyaline inclusions in motor neurons. Arch Neurol 27:292–299

39. Wood ZA, Poole LB, Karplus PA (2003) Peroxiredoxin evolution and the regulation of hydrogen peroxide signaling. Science 300:650–653

ELSEVIER

Neuroprotective effect of oxidized galectin-1 in a transgenic mouse model of amyotrophic lateral sclerosis

Ren Chang-Hong[a], Manabu Wada[a,*], Shingo Koyama[a], Hideki Kimura[a], Shigeki Arawaka[a], Toru Kawanami[a], Keiji Kurita[a], Toshihiko Kadoya[b], Masashi Aoki[c], Yasuto Itoyama[c], Takeo Kato[a]

[a]*Department of Neurology, Hematology, Metabolism, Endocrinology and Diabetology, Yamagata University School of Medicine, 2-2-2 Iida-Nishi, Yamagata 990-9585, Japan*
[b]*Pharmaceutical Research Laboratory, Kirin Brewery Company, Ltd., Takasaki, Japan*
[c]*Department of Neurology, Tohoku University School of Medicine, Sendai, Japan*

Abstract

Abnormal accumulation of neurofilaments in motor neurons is a characteristic pathological finding in amyotrophic lateral sclerosis (ALS). Recently, we revealed that galectin-1, whose oxidized form has axonal regeneration-enhancing activity, accumulates in the neurofilamentous lesions in ALS. To investigate whether oxidized galectin-1 has a beneficial effect on ALS, oxidized recombinant human galectin-1 (rhGAL-1/ox) or physiological saline was injected into the left gastrocnemius muscle of the transgenic mice over-expressing a mutant copper/zinc superoxide dismutase (SOD1) with a substitution of histidine to arginine at position 46 (H46R SOD1). The H46R SOD1 transgenic mice, which represented a new animal model of familial ALS, were subsequently assessed for their disease onset, life span, duration of illness, and motor function. Furthermore, the number of remaining large anterior horn cells of spinal cords was also compared between the two groups. The results showed that administration of rhGAL-1/ox to the mice delayed the onset of their disease and prolonged the life of the mice and the duration of their illness. Motor function, as evaluated by a Rotarod performance, was improved in rhGAL-1/ox-treated mice. Significantly more anterior horn neurons of the lumbar and cervical cords were preserved in the mice injected with rhGAL-1/ox than in those injected with physiological saline. The study suggests that rhGAL-1/ox administration could be a new therapeutic strategy for ALS.
© 2005 Elsevier Inc. All rights reserved.

Keywords: Amyotrophic lateral sclerosis; Oxidized galectin-1; Cu/Zn superoxide dismutase; Transgenic mice

Introduction

Amyotrophic lateral sclerosis (ALS) is a fatal neurodegenerative disease characterized by loss of motor neurons in the cerebral motor cortex, brainstem, and spinal cord. ALS shows progressive muscle weakness and atrophy, with most patients dying within 5 years of disease onset (Cleveland, 1999; Rowland and Schneider, 2001). Usually, ALS occurs sporadically; however, approximately 10% of ALS cases show an autosomal dominant inheritance. Of these patients with familial ALS (FALS), 10–20% have missense mutations or a small deletion of the gene encoding Cu/Zn superoxide dismutase (SOD1) (Cleveland, 1999; Rowland and Schneider, 2001). Several lines of transgenic (Tg) mice with a FALS-linked mutated SOD1 gene have been made, and these mice have developed an adult onset paralytic disorder that is similar to sporadic and familial ALS (Bruijn et al., 1998; Gurney et al., 1994; Ripps et al., 1995; Tu et al., 1996). Accordingly, those Tg mice with SOD1 mutations have been used as an animal model for ALS.

Immunohistochemical investigations of the ALS spinal cord have shown that an abnormal accumulation of neuro-

---

filaments in the cytoplasm and cell processes is a common pathological hallmark of both sporadic and familial ALS (Cleveland, 1999). The abnormal accumulation of neurofilaments induces axonal spheroids, cord-like neurite swellings, and perikaryal conglomerate inclusions in degenerating motor neurons of the spinal cord. These pathological features are considered to be important early pathological changes in ALS (Hirano et al., 1984; Kato et al., 2001). Therefore, an investigation of the accumulation of neurofilaments may help to understand the pathogenesis of motor neuron degeneration in ALS.

We have previously reported that galectin-1, which is a member of the β (beta)-galactoside-binding lectins, is accumulated in neurofilamentous lesions of the spinal cord in both sporadic and familial ALS (Kato et al., 2001). Galectin-1 has been shown to take two molecular forms: oxidized and reduced (Inagaki et al., 2000). Since oxidized galectin-1 has been reported to promote axonal regeneration after a peripheral nerve injury (Fukaya et al., 2003; Horie and Kadoya, 2000; Horie et al., 1999; Inagaki et al., 2000), it is possible that oxidized galectin-1 promotes the survival of the degenerating motor neurons in ALS.

The Tg mice expressing mutant human SOD1 with a substitution of histidine to arginine at position 46 (H46R SOD1) were established as a new animal model of familial ALS. In the present investigation, we administered oxidized galectin-1 to the H46R SOD1 Tg mice and subsequently assessed their disease onset, life span, duration of illness, and motor function. The present study showed that oxidized galectin-1 had a beneficial effect on the motor function and survival of Tg mice. This is the first report of a possible therapeutic effect of oxidized galectin-1 on ALS.

Materials and methods

Construction of transgenic (Tg) mice expressing mutant human SOD1

The present study was performed on Tg mice expressing mutant human SOD1 with a substitution of histidine to arginine at position 46 (H46R SOD1). We isolated a clone containing the full genomic human SOD1 gene, which was identified by screening a human genomic PAC library (Ioannou et al., 1994) using PCR with pairs specific to the human SOD1 gene. Subsequently, we cloned an 11.5 kb EcoRI–BamHI fragment that contained the entire coding sequence and promoter region of the human SOD1 gene (Elroy-Stein et al., 1986; Levanon et al., 1985). The H46R mutation was engineered into this fragment by site-directed mutagenesis (Mutan-express Km, Takara, Otsu, Japan). The mutagenic primer and selection primer, which restored the Km resistance, hybridized to the vector and were incorporated during replication. The resulting potential Km resistant clone was subsequently sequenced (oligonucleotide-directed dual amber method) (Hashimoto-Gotoh et al.,

1995) to verify the presence of either of the introduced mutations.

A linear 11.5 kb EcoRI–BamHI fragment containing the H46R mutation was microinjected into BDF1 (C57BL/6 × DBA/2 F1) mouse (Jackson Laboratories, Bar Harbor, ME) embryos. The treated embryos were subsequently transferred to the oviducts of pseudopregnant ICR-scl female mice. The male littermates that were heterozygous for the H46R SOD1 mutation were used in this study. The mutated H46R SOD1 gene was identified by tail-clip PCR amplification using human SOD1-specific primers (sense primer: 5′-TTGGGAGGAGGTAGTGATTA-3′ and anti-sense primer: 5′-AGCTAGCAGGATAACAGATGA-3′). PCR was conducted with 1 cycle at 94°C for 2 min followed by 25 cycles at 94°C for 30 s, 58°C for 30 s, and 72°C for 30 s. Founder mice were then mated with C57B/6 mice (Jackson Laboratories).

Histopathological and immunohistochemical analysis

The mice were anesthetized with diethyl ether and killed by transcardiac perfusion with physiological saline followed by 4% paraformaldehyde containing phosphate-buffered saline (PBS; pH 7.4). The spinal cord was removed, post-fixed in the above solution, and embedded in paraffin. Serial transverse sections (4 μm thickness) of the lumbar segment (L_{4-5}) were cut and stained with hematoxylin and eosin (H&E) for a routine histological investigation. Several sections were also used for immunohistochemical investigations. Immunohistochemistry was performed using antibodies against human SOD1 (dilution 1:500, MBL, Japan), ubiquitin (dilution 1:100, DAKO, Denmark), and glial fibrillary acidic protein (GFAP; dilution 1:500, DAKO, Denmark). Deparaffinized sections were incubated with 1% H_2O_2 in distilled water for 10 min followed by 5% normal goat serum. The sections were subsequently incubated with primary antibodies in PBS containing 0.03% Triton X-100 at 4°C for 48 h. They were then incubated with a biotinylated secondary antibody (Vector, Burlingame, CA) for 2 h. After incubation with the avidin–biotin–peroxidase complex (ABC; Vector) for 1 h, peroxidase labeling was visualized by incubating the sections with 0.05 M Tris-buffered saline containing 0.05% 3,3′-diaminobenzidine tetrahydrochloride (DAB), 0.05 M imidazole, and 0.00015% H_2O_2 to yield a brown reaction product. The sections were then counter-stained with hematoxylin. Non-Tg mice were used for a comparison of histological findings.

Preparation of oxidized recombinant human galectin-1 (rhGAL-1/ox)

rhGAL-1/ox was obtained according to previous methods (Inagaki et al., 2000). In brief, rhGAL-1 was expressed in Escherichia coli and purified from the supernatant of the sonicated E. coli by DEAE-HPLC. Oxidized galectin-1

was obtained from bacterially expressed rhGAL-1 by the air oxidation method with $CuSO_4$ as a catalyst. DEAE-purified rhGAL-1 was subsequently diluted 20-fold with 20 mM Tris–HCl, pH 8.0, $CuSO_4$ was added to a final concentration of 0.0001% (w/v), and the mixture was maintained overnight at 4°C to allow disulfide bound formation.

rhGAL-1/ox was then purified by reversed-phase HPLC on a YMC-pack Protein RP column (YMC) with a linear gradient of acetonitrile in 0.1% trifluoroacetic acid. The purified rhGAL-1/ox contains three intramolecular disulfide linkages between Cys^2 and Cys^{130}, Cys^{16} and Cys^{88}, and Cys^{42} and Cys^{60}, which represent a stable conformation of oxidized galectin-1. Analysis by SDS-PAGE and HPLC revealed that rhGAL-1/ox was not degenerated even after 10 days of incubation at 37°C in PBS (5 μl protein/ml). rhGAL-1/ox confirmed that the protein promotes axonal regeneration in both the in vitro examination (Horie et al., 2004) and in the in vivo acellular nerve regeneration model (Fukaya et al., 2003).

Experimental protocol

Kadoya et al. recently reported that the application of rhGAL-1/ox (0.125 μg/body weight (g)/week) to the injured region promotes the restoration of nerve function using in vivo peripheral nerve regeneration model (Kadoya et al., in press). No one showed any toxic effects in reaction to the administration of rhGAL-1/ox. The concentration of rhGAL-1/ox in the present study was chosen because previous investigation demonstrated the effect and safety in an animal model and because a higher dose would be expected to promote the survival of the degenerating motor neurons. For the reasons above, 0.25 μg/g (body weight)/week of rhGAL-1/ox was administered to the H46R SOD1 Tg mice. Furthermore, intramuscular administration of rhGAL-1/ox was performed on a weekly basis in considering the application of rhGAL-1/ox to human ALS in the future.

The Tg mouse littermates were randomly divided into two groups: (1) administration of rhGAL-1/ox of 0.25 μg/g (body weight) (gal-1-treated group); and (2) administration of 60 μl physiological saline (control group). rhGAL-1/ox was diluted with physiological saline and injected into the left gastrocnemius muscle using a microsyringe connected to a 27-gauge needle. The control group received physiological saline instead of rhGAL-1/ox. To clarify whether rhGAL-1/ox delays the onset of the disease, intramuscular injection was started prior to the early presymptomatic stage. At postnatal day 70 (10 weeks of age), the mice started receiving a weekly intramuscular injection of rhGAL-1/ox or physiological saline. Twenty-eight transgenic mice (gal-1-treated group, $n = 14$; control group, $n = 14$) were used for the assessment of disease onset, life span, and duration of illness. Among them, 19 transgenic mice (gal-1-treated group, $n = 10$; control

group, $n = 9$) were used for the assessment of motor function. Additional transgenic mice (gal-1-treated group, $n = 6$; control group, $n = 5$) were used for the histological and pathological investigation.

Assessment of motor function

Motor function was assessed using a Rotarod (Muromachi Instruments, Tokyo, Japan) on a weekly basis. The period for which a mouse could remain on a rotating axle (diameter, 30 mm; two sets of rotation speed, 5 and 20 rpm) without falling was measured. The time was automatically stopped if the mouse fell from the rod or after an arbitrary limit of 420 s (Li et al., 2000). Mice were tested once a week until they could no longer perform the task. An examiner who was blinded to the experimental design assessed the motor functions of the mice mentioned above. The onset of motor dysfunction was defined as the first day when a mouse could not remain on the Rotarod for 420 s at a speed of 20 rpm, as described previously (Li et al., 2000). The life span was defined as the postnatal day when the mouse died (Shefner et al., 2001). The duration of illness was defined as the number of days from the onset of motor dysfunction to death (Wang et al., 2002).

Assessment of body weights with transgenic mice

The body weight of each transgenic mouse was assessed on a weekly basis. Twenty-eight transgenic mice (gal-1-treated group, $n = 14$; control group, $n = 14$), which were used for the assessment of survival, were also used for the assessment of body weights.

Histopathological examination: tissue preparation and cell counting

The mice, which had been anesthetized with diethyl ether, were sacrificed by transcardiac perfusion with physiological saline followed by 4% paraformaldehyde containing PBS (pH 7.4). The spinal cord was removed, post-fixed in the above solution, and embedded in paraffin. Serial transverse sections (4 μm thickness) of the lumbar segment ($L_{4–5}$) were cut and stained with H&E for a routine histological investigation.

The number of spinal anterior horn neurons was examined at postnatal day 147 (21 weeks of age). Thirty serial sections each (10 μm thickness) of the cervical ($C_{5–6}$) and the lumbar cords ($L_{4–5}$) were stained by the Nissl method and photographed under light microscopy at 40× magnification. An examiner who was blinded to the experimental design counted the anterior horn cells that met all of the following criteria: (1) neurons located in the anterior horn ventral to the line tangential to the ventral tip of the central canal; (2) neurons with a maximum diameter of 20 μm or more; and (3) neurons with a distinct nucleolus (Manabe et al., 2003; Warita et al., 1999).

Statistical analysis

For the two groups, the disease onset, length of survival, and duration of illness were evaluated using the Log-rank. The results of motor function tested with the Rotarod and the body weights of transgenic mice were statistically analyzed using ANOVA for multiple comparisons among the groups. The number of anterior horn neurons in each group was compared using the two-tailed Student's *t* test. Statistical analysis was performed using computerized software (SPSS ver. 11.0, Chicago, Illinois, USA). $P < 0.05$ was accepted as statistically significant.

The experiment was approved by the Committee on Ethics of Animal Experiments and followed the Yamagata University School of Medicine Guidelines for Animal Experiments.

Results

Clinical phenotype and course of the transgenic mice

All the mice used had H46R mutant SOD1, as demonstrated by tail-clip PCR. These mice presented motor dysfunction similar to human ALS; the first sign of disease was weakness in their hind limbs, mostly shown by dragging of one limb. As the disease progressed, the mice showed marked muscle wasting in their limbs. The other muscles also became weak; thereafter, the affected mice could not move to reach their water supply and died. The

motor dysfunction occurred at about 20 weeks of age, and most mice died at about 24 weeks of age.

Histopathological and immunohistochemical studies in the spinal cords

In mice at the early presymptomatic stage (91 days of age), no apparent changes were observed in the H&E-stained sections (Fig. 1A). Small numbers of GFAP-immunoreactive astrocytes were seen (Fig. 1E). At the late presymptomatic stage (119 days of age), large anterior horn cells seemed to decrease in number (Fig. 1B). By 147 days of age (the early symptomatic stage), when weakness of the limbs became apparent, there was a marked loss in the number of anterior horn cells (Fig. 1C) accompanied by astrocytic proliferation (Fig. 1G). Neurite swellings in the anterior horns were also observed (Fig. 2B). Eosinophilic inclusion bodies similar to Lewy body-like hyaline inclusions in human ALS were detectable in the anterior horns. These inclusions were immunostained with anti-SOD1 antibody and anti-ubiquitin antibody, most of which were detected in the neuropil (Figs. 2A and C), and only a few were within the perikarya of neurons (Fig. 2D). At the end stage, there was a severe decrease in the number of anterior horn neurons (Fig. 1D) with diffuse astrocytic proliferation (Fig. 1H). There were no remarkable vacuoles like those in cell bodies, dendrites, and axons of previously reported transgenic mice expressing SOD1 mutation G37R (Wong et al., 1995) or G93A (Gurney et al., 1994).
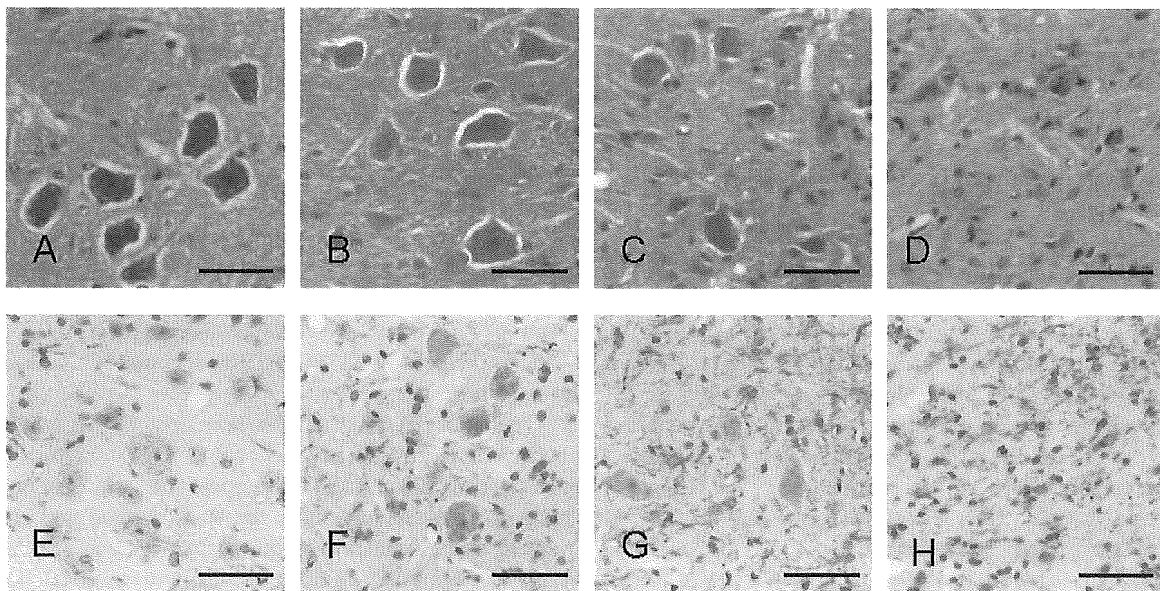

Fig. 1. Histopathological findings of the lumbar cord in the H46R transgenic mice. Sections were stained with hematoxylin–eosin (H&E) (A–D) and immunostained with anti-glial fibrillary acidic protein (GFAP) antibody (E–H). (A, E) No apparent changes are observed in the section stained with H&E in the early presymptomatic stage (91 days of age). Small numbers of GFAP-immunoreactive astrocytes are seen. (B, F) The number of large anterior horn cells seems to decrease in the late presymptomatic stage (119 days of age) accompanied by astrocytic proliferation. (C, G) A marked loss of anterior horn cells is seen with an increase in the number of astrocytes at the early symptomatic stage (147 days of age). (D, H) A severe loss of anterior horn neurons is observed at the end stage (168 days of age). Scale bars = 50 μm.
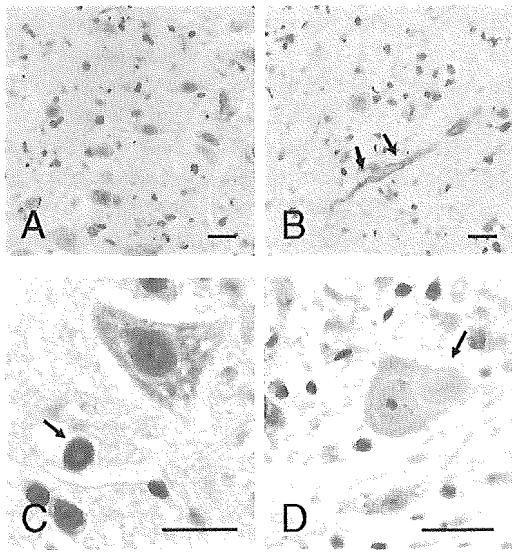
Fig. 2. (A) Many inclusion bodies, immunostained with anti-ubiquitin antibody, are readily apparent in the neuropil of the spinal ventral horn. (B) Cord-like neurite thickening of the ventral horn is immunostained with anti-ubiquitin antibody. (C) A Lewy body-like inclusion in neuropil is immunostained with anti-ubiquitin antibody. (D) A Lewy body-like inclusion immunostained with anti-SOD1 antibody is seen in the spinal anterior horn neuron. Scale bars = 20 μm.

Effects of rhGAL-1/ox on the disease course

rhGAL-1/ox delayed the onset of disease

The onset of the disease, as defined by falling from the Rotarod (20 rpm) within 420 s, occurred at postnatal day 138.3 ± 1.7 in the control group. The gal-1-treated mice showed a statistically significant delay of onset (postnatal day 143.5 ± 1.5) ($P = 0.0156$) (Fig. 3A and Table 1).

rhGAL-1/ox prolonged survival

The life span was much longer (172.2 ± 1.3 days) in the mice in the gal-1-treated group than in those in the control group (160.4 ± 2.4 days) ($P < 0.0001$) (Fig. 3B and Table 1).

rhGAL-1/ox prolonged the duration of illness

The duration of illness was significantly longer in the mice in the gal-1-treated group (28.7 ± 1.8 days) than in those in the control group (22.1 ± 1.4 days) ($P = 0.0072$) (Table 1).

rhGAL-1/ox improved motor function

In the condition with 5 rpm, which was a weak task, differences in motor function between the two groups were not apparent at postnatal day 133 (19 weeks of age). Although motor function appeared to be better in the mice in the gal-1-treated group than in those in the control group at the early symptomatic stage, the difference between two groups was not statistically significant (ANOVA; $P = 0.282$) (Fig. 4A).
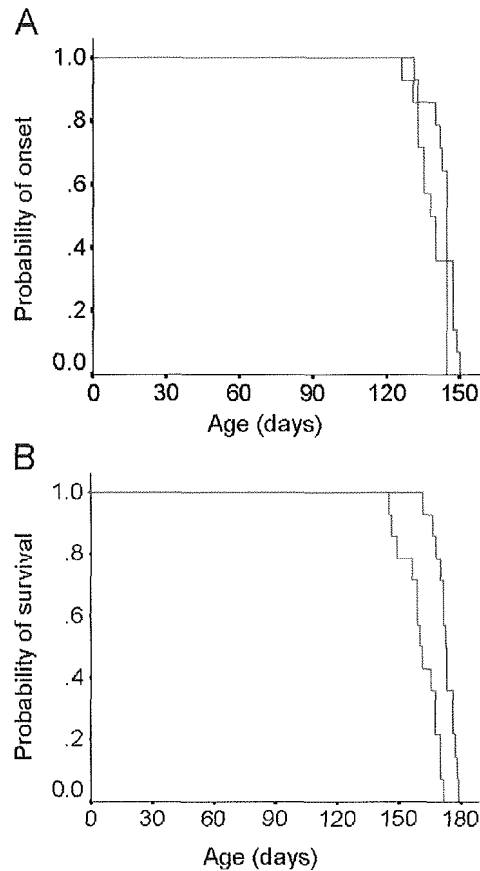

Fig. 3. rhGAL-1/ox delayed the disease onset and prolonged the survival of Tg mice (mutant H46R SOD1). The Kaplan–Meier curves demonstrate the probability of onset of Rotarod deficit (A) and length of survival (B) in Tg mice (mutant H46R SOD1). The onset of the Rotarod deficit was more delayed in the gal-1-treated group than it was in the control group ($P = 0.0156$) (A). The life span was significantly more prolonged in the gal-1-treated group than in the control group ($P < 0.0001$) (B). Red line, gal-1 group ($n = 14$); blue line, control group ($n = 14$).

In the condition with 20 rpm, which corresponded to a heavy task, motor function was better in the gal-1-treated mice than in the control group mice at postnatal day 103 (19 weeks of age). The motor function of the mice in the gal-1-treated group was significantly better than that in the mice in the control group ($P = 0.038$) (Fig. 4B).

The body weight changes of the transgenic mice

At the end stage (168 days of age), the mice in the control group showed a body weight loss by 7%, compared

Table 1
Onset of motor dysfunction, survival, and duration of illness

	Control ($n = 14$)	Gal-1 ($n = 14$)	P value
Onset (postnatal days)	138.3 ± 1.7	143.5 ± 1.5	0.0156
Survival (days)	160.4 ± 2.4	172.2 ± 1.3	<0.0001
Duration (days)	22.1 ± 1.4	28.7 ± 1.8	0.0072

Values tabulated are mean ± SEM. Statistical comparisons were with Log-rank test.